Biofilm 9 (2025) 100279

Contents lists available at ScienceDirect

Biofilm

journal homepage: www.sciencedirect.com/journal/biofilm

Modeling reciprocal adaptation of *Staphylococcus aureus* and *Pseudomonas aeruginosa* co-isolates in artificial sputum medium

Zhifen Wang [a,#], Emily Giedraitis [b], Christiane Knoop [c], Daniel J. Breiner [b], Vanessa V. Phelan [b,1], Françoise Van Bambeke [a,*,1]

[a] Pharmacologie Cellulaire et moléculaire, Louvain Drug Research Institute, Université Catholique de Louvain, Brussels, Belgium
[b] Department of Pharmaceutical Sciences, Skaggs School of Pharmacy and Pharmaceutical Sciences, University of Colorado Anschutz Medical Campus, Aurora, CO, USA
[c] Erasme Hospital, Université libre de Bruxelles, Brussels, Belgium

ARTICLE INFO

Keywords:
Cystic fibrosis
Dual-species
Biofilm
Staphylococcus aureus
Pseudomonas aeruginosa
Artificial sputum medium

ABSTRACT

Co-infections by *Staphylococcus aureus* and *Pseudomonas aeruginosa* are frequent in the airways of patients with cystic fibrosis. These co-infections show higher antibiotic tolerance *in vitro* compared to mono-infections. *In vitro* models have been developed to study the interspecies interactions between *P. aeruginosa* and *S. aureus*. However, these model systems fail to incorporate clinical isolates with diverse phenotypes, do not reflect the nutritional environment of the CF airway mucus, and/or do not model the biofilm mode of growth observed in the CF airways. Here, we established a dual-species biofilm model grown in artificial sputum medium, where *S. aureus* was inoculated before *P. aeruginosa* to facilitate the maintenance of both species over time. It was successfully applied to ten pairs of clinical isolates exhibiting different phenotypes. Co-isolates from individual patients led to robust, stable co-cultures, supporting the theory of cross-adaptation *in vivo*. Investigation into the cross-adaptation of the VBB496 co-isolate pair revealed that both the *P. aeruginosa* and *S. aureus* isolates had reduced antagonism, in part due to reduced production of *P. aeruginosa* secondary metabolites as well as higher tolerance to those metabolites by *S. aureus*. Together, these results indicate that the two-species biofilm model system provides a useful tool for exploring interspecies interactions of *P. aeruginosa* and *S. aureus* in the context of CF airway infections.

1. Introduction

Cystic Fibrosis (CF) is an autosomal genetic disease caused by mutations in the cystic fibrosis transmembrane conductance regulator (CFTR) gene encoding the epithelial ion channel that normally transports chloride and bicarbonate [1]. Mutations in CFTR lead to the accumulation of thick mucus in airways of patients with CF [2], which is a beneficial niche for colonization by multiple bacteria. Among them, *Staphylococcus aureus* and *Pseudomonas aeruginosa* are the most prevalent [3].

S. aureus is predominant in children and adolescents (present in 80 % of patients) while *P. aeruginosa* is more prevalent in adults (present in 70 % of patients) [3]. Due to the shift in microbial abundance from *S. aureus*-dominant to *P. aeruginosa*-dominant through adolescence into adulthood, it was hypothesized that a succession event occurs whereby *P. aeruginosa* displaces *S. aureus* within the CF airway over time [4–10]. Yet, both species are isolated concomitantly from the sputum of 20–30 % of the patients with CF [3] and were stably recovered from sputum cultures over the span of 10 years [11]. Co-infection of the CF airways with *P. aeruginosa* and *S. aureus* has been correlated in some studies with worsened clinical outcomes. Although a causality relationship has not been established, the studies suggest that co-infections are more virulent [12], associated with higher rates of morbidity and mortality [13,14], and complicate antibiotic treatment compared to mono-infection [15].

Despite co-existing in the CF airway, antagonism between *P. aeruginosa* and *S. aureus* is often observed *in vitro*, with *P. aeruginosa* readily outcompeting *S. aureus* [6,16,17]. These observations are due, in part, to model systems that fail to reflect the *in vivo* environment. Most co-culture studies of these two pathogens use reference strains [16,18,19], despite experimental evidence indicating that *P. aeruginosa* clinical

* Corresponding author. Avenue Mounier 73 B1.73.05, 1200, Brussels, Belgium.
E-mail address: francoise.vanbambeke@uclouvain.be (F. Van Bambeke).
current affiliation: Department of Pharmacy, The Affiliated Hospital of Guizhou Medical University, Guiyang 550,004, China.
[1] equal contribution as last authors.

https://doi.org/10.1016/j.bioflm.2025.100279
Received 19 January 2025; Received in revised form 1 April 2025; Accepted 7 April 2025
Available online 11 April 2025

isolates are less antagonistic to *S. aureus*. Additionally, studies are often performed in standard laboratory media [16,20,21] rather than physiologically relevant nutrient conditions reflective of the CF airways [22–24]. Moreover, many studies are performed using planktonic cultures. However, in the CF airways, both *S. aureus* and *P. aeruginosa* grow as biofilms, defined as microbial aggregates encased by a self-produced extracellular matrix. *In vitro,* this matrix is mainly composed of proteins, exopolysaccharides (EPS), and environmental DNA [25], but has not been characterized *in vivo*. In addition to reducing the penetrance of antimicrobials and ability of the immune system to clear the infection, the biofilm mode of growth is characterized by heterogeneous metabolism [26,27].

The aim of this study was to develop and implement an *S. aureus* and *P. aeruginosa* dual-species biofilm model grown in an artificial sputum medium previously shown to mimic the viscoelastic properties of the mucus of patients with CF [28]. In the CF airway, *P. aeruginosa* and *S. aureus* likely occupy the same niche [29,30], but may form spatially segregated biofilms analogous to those observed in wounds [31]. In this model system, we compared the growth, biofilm formation, aggregation, and chemical interactions of reference strains with clinical isolates collected in pairs from patients with CF. In brief, we show that co-cultures of co-isolated *P. aeruginosa* and *S. aureus* were more stable compared to reference strains and we identify several factors that contribute to cross adaptation of *S. aureus* and *P. aeruginosa*.

2. Materials and methods

2.1. Laboratory strains and clinical isolates

Laboratory strains *P. aeruginosa* PAO1 and *S. aureus* ATCC25923 were selected as reference strains. Ten pairs of *S. aureus* and *P. aeruginosa* were collected as routine samples and isolated concomitantly from bronchopulmonary sputum of seven CF patients (Table 1).

2.2. Artificial sputum medium

Artificial sputum medium (ASM+) was prepared as reported by Diaz Iglesias et al. [28,32], with the following modifications: agar was purchased from Sigma-Aldrich (St Louis, MO) and pH was adjusted to a range of 7.1–7.4 with 0.2 N of NaOH. The prepared ASM+ was stored at 4 °C for a fortnight and thoroughly homogenized by agitation before use. It was used within 2 months.

Table 1
Identification of clinical isolates and phenotype of *P. aeruginosa*.

Isolate ID	Date of isolation	Specific isolates[a]	Name of the corresponding pair
857JBJ	08.04.2021	Sa 857JBJ	857JBJ
		Pa 857JBJ (pigmented non-mucoid)	
UEQ307	25.03.2021	Sa UEQ307	UEQ307-3
		Pa UEQ307-3 (pigmented non-mucoid)	
		Pa UEQ307-4 (pigmented non-mucoid)	UEQ307-4
		Pa UEQ307-5 (pigmented non-mucoid)	UEQ307-5
UEQ310	29.03.2021	Sa UEQ310	UEQ310
		Pa UEQ310 (pigmented mucoid)	
VBB496	12.04.2021	Sa VBB496	VBB496
		Pa VBB496 (non-pigmented mucoid)	
492IVJ	29.03.2021	Sa 492IVJ	492IVJ
		Pa 492IVJ (non-pigmented mucoid)	
UEQ301	15.03.2021	Sa UEQ301	UEQ301
		Pa UEQ301 (non-pigmented mucoid)	
UEQ306	25.03.2021	Sa UEQ306	UEQ306-2
		Pa UEQ306-2 (SCV)	
		Pa UEQ306-3 (SCV)	UEQ306-3

[a] Sa: *S. aureus*; Pa : *P. aeruginosa*.

2.3. Development of dual-species biofilms

S. aureus or *P. aeruginosa* were suspended in cation-adjusted Mueller Hinton Broth (MHB-Ca; Sigma-Aldrich) from overnight cultures on Trypticase soy agar (TSA; VWR) and adjusted to an optical density (OD) at 620 nm of 0.5 (or 2.6 McFarland units). Subsequently, *S. aureus* was diluted 10-fold in MHB-Ca (final inoculum: 2.1×10^7 CFU/mL), and *P. aeruginosa*, 20- (1.35×10^7 CFU/mL), 200- (1.35×10^6 CFU/mL), or 1000-fold (2.7×10^5 CFU/mL) in MHB-Ca.

For dual-species biofilm protocol #1 [33], *S. aureus* at 2.1×10^7 CFU/mL and *P. aeruginosa* at each dilution were mixed at equivalent volume. Subsequently, 200 μL of the mixed *S. aureus* - *P. aeruginosa* suspensions (1:0.64; 1:0.064; and 1:0.013 final Sa:Pa ratios) were inoculated in the wells of 96-well polystyrene plates (VWR) and incubated for 2 h to favor attachment, after which MHB-Ca was replaced by ASM+, and cultures were incubated for 24, 48, or 72 h, with daily refreshment of the medium.

In dual-species biofilm protocol #2 [16], 200 μL of *S. aureus* (approx. 2.1×10^7 CFU/mL) was inoculated in the wells of 96-well polystyrene plates and incubated for 2 h to allow attachment. MHB-Ca was then replaced with ASM+, and the *S. aureus* was further incubated for 24 h. Afterward, the ASM+ was removed, and 20 μL of *P. aeruginosa* at 1.35×10^7 or 2.7×10^6 CFU/mL were added to the pre-established *S. aureus* biofilm. An additional 180 μL of ASM+ was then added to each well, bringing a final volume to 200 μL. These ratios represent 1:0.064 and 1:0.013 Sa:Pa CFU/mL. ASM+ was renewed every 24 h up to 120 h (5 days). Medium removal was performed using a multi-channel pipette. To ensure minimal disturbance to surface-attached bacteria, the pipette tips were positioned at a 45° angle near the bottom of each well. Complete removal of the spent medium was achieved through gentle, sequential aspiration of small volumes (typically 50–100 μL per cycle). This general protocol was also applied to co-cultures of clinical isolates of cross cultures, using the 1:0.064 Sa:Pa CFU/mL ratio and applied for subsequent experiments.

2.4. Quantification of viability

Viability was quantified by cell counting (CFU/mL). Surface attached cells were washed once with sterile phosphate buffer saline (PBS) and mechanically disrupted using the tip of a disposable bacterial inoculation loop followed by resuspension in 200 μL PBS and sonication for 30 s at 60 % amplitude using a Q700 sonicator (QSonica). Resuspended bacteria were diluted 10 to 10^6 times in PBS, and 50 μL were plated on Mannitol Salt Agar (MSA) for *S. aureus* or Pseudomonas Isolation Agar (PIA) for *P. aeruginosa*. CFU were counted after the minimum amount of time required for sufficient growth and accurate counting of *S. aureus* and *P. aeruginosa*.

2.5. Quantification of biofilm biomass

For estimation of the total biomass, the washed biofilms were dried at 60 °C for at least 24 h, and 0.5 % (v/v) crystal violet (100 %, Sigma-Aldrich) in water was added to 96-well plates (200 μL/well) [34]. The plates were incubated for 10 min at room temperature, non-bound crystal violet was discarded by inversion of plates and the stained biofilm was rinsed with running water, after which bound crystal violet was re-solubilized in 200 μL of 66 % (v/v) acetic acid and incubated 1 h in the dark. Biofilm biomass was quantified by measuring crystal violet absorbance at 570 nm in a SpectraMax M3 plate reader (Molecular Devices LLC). Wells containing only ASM were used as blanks, and the absorbance measured in these wells removed from all values.

2.6. Confocal laser scanning microscopy of S. aureus and P. aeruginosa co-cultures

Dual-species biofilms were grown for 72 h according to protocol #2 on 12 mm coverslips placed in 24-well polystyrene plates (equivalent volume scaling). In brief, 1000 μL of *S. aureus* (approx. 2.1×10^7 CFU/mL) was inoculated on coverslips placed in 24-well plates and incubated for 2 h in MHB-Ca to allow attachment, then the MHB-Ca was removed, and the coverslip was incubated for an additional 24 h in ASM+. After incubation, the medium was removed, and 100 μL of *P. aeruginosa* (approx. 1.35×10^7 CFU/mL) was added to the pre-established *S. aureus* biofilm, and 900 μL of ASM+ was replenished to reach a volume of 1000 μL. After 72 h, biofilms were washed once in PBS and fixed with 4 % formaldehyde in PBS for 1 h at room temperature. The fixed biofilms were incubated in pre-heated permeabilization reagent (1000 μL per well) (Tris-HCl 20 mM, EDTA 5 mM, lysozyme 1 mg/mL (Sigma-Aldrich), lysostaphin 0.1 mg/mL (Sigma-Aldrich), pH 7.7) for 10 min at 37 °C, after which hybridization buffer (Tris-HCl 20 mM, NaCl 900 mM, SDS 0.1 mg/L, formamide 20 % (v/v), pH 7.7) without DNA-probe was added and incubated for 15 min at 46 °C [35]. Then, the biofilm was hybridized with *S. aureus*-specific (5′-Cy5-TCC TCC ATA TCT CTG CGC-3' [36]) and *P. aeruginosa*-specific (5′-Atto 488-GGT AAC CGT CCC CCT TGC-3' [37]) DNA-FISH probes for 3 h at 47 °C in darkness. Non-bound probes were removed by incubation in washing buffer (Tris-HCl 20 mM, EDTA 5 mM, SDS 0.1 mg/L, NaCl 450 mM, pH 7.7) for 15 min at 46 °C. The coverslips were mounted by inversion on a 100 mm glass microscope slide with DAKA mounting oil. The stained dual-species biofilms were observed in an inverted cell observation spinning disk microscope (Carl Zeiss) with an oil immersion 40 × objective. *P. aeruginosa* targeted by PA-Atto 488 was detected in the green channel (excitation/emission, 488/533 nm), and *S. aureus* targeted by Sa-cy5, in the red channel (excitation/emission, 633/678 nm), and biofilms were analyzed using Z-stacks scanning model. 3D-images of biofilms were obtained using the ZEN 2.6 (blue edition) software.

2.7. Quantitative reverse transcription PCR analysis

The relative gene expression of *sigB*, *icaA*, *clfA*, and *spa* of *S. aureus* VBB496 and *lasI*, *pvdS*, *pqsL*, *acoR*, and *PA4148* of *P. aeruginosa* VBB496 was analyzed in biofilms comprised of VBB496 co-isolates or cross-culture with the reference strains (see primers in Table S1). Dual-species biofilms were incubated in 96-well polystyrene plates using Protocol #2 with an inoculum ratio of 1 Sa to 0.064 Pa. After 72 h of incubation, surface-attached biofilms were washed once in PBS and recovered by vigorous pipetting. Samples were pooled (2 mL) in tubes and centrifuged at 10,000 g for 15 min at 4 °C, after which the pellet was suspended in an appropriate volume of PBS, then transferred to a new tube and centrifuged at 10,000 g for 10 min. The pellet was treated with 300 μL of 3 mg/mL lysozyme in TE buffer (Tris-HCl 10 mM, EDTA 1 mM (ThermoFisher Scientific) at pH 8.0) for 30 min at room temperature. When *S. aureus* was present in the sample, a final concentration of 100 μg/mL lysostaphin (Sigma Aldrich) was added. Total RNA was extracted from dual-species biofilms using the Invitrap Spin Cell RNA mini kit (Invitek Molecular) according to the manufacturer's instructions, followed by DNase (TURBO DNA-free kit, Thermofisher Scientific) treatment 30 min cDNA synthesis was performed using the First Strand cDNA Synthesis kit (Roche, Basel, Switzerland) following the manufacturer's instructions. The relative quantification of cDNA was performed by real-time PCR with detection by SYBR Green Supermix (Bio-Rad). Data were expressed as the relative fold change in gene expression of the co-isolate VBB496 pair to the appropriate cross-strain pair determined via $2^{-\Delta\Delta CT}$ method [38] using *gmk* and 16s-RNA as housekeeping genes for *S. aureus* and *P. aeruginosa*, respectively.

2.8. Metabolomics analysis of P. aeruginosa exoproducts

Mono- and dual-species cultures were grown using the procedures outlined in Protocol #2, with a ratio of 1 Sa to 0.064 Pa for the dual-species culture. At 48, 72, and 96 h, ASM+ was removed, then surface-attached biofilms were mechanically disrupted and homogenized by pipetting up and down. The resulting suspensions were transferred into 96-well polypropylene plates (100 μL per well), supplemented with 10 μM nalidixic acid as an internal standard, and chemically disrupted using an equal volume of 1:1 ethyl acetate (EtOAc, VWR HiperSolv Chromanorm) and methanol (MeOH, Fisher Scientific Optima-grade), followed by 10 min of sonication in a water bath sonicator. All samples were dried overnight in a chemical hood and stored at −20 °C until use. Samples were resuspended in 100 % MeOH containing 1 μM glycocholic acid (Calbiochem; 100.1 % pure). Mass spectrometry data acquisition was performed using a Bruker Daltonics Maxis II HD quadrupole time of flight (qTOF) mass spectrometer equipped with a standard electrospray ionization (ESI) source as previously described [39]. Briefly, the mass spectrometer was tuned by infusion of tuning mix ESI-TOF (Agilent Technologies) at a 3-ml/min flow rate. For accurate mass measurements, a wick saturated with hexakis (1H,1H,2H-difluoroethoxy) phosphazene ions (Apollo Scientific, *m/z* 622.1978) located within the source was used as a lock mass internal calibrant. Samples were introduced by an Agilent 1290 ultraperformance liquid chromatography (UPLC) system. Optima-grade (Fisher Scientific) acetonitrile (ACN), formic acid (FA), and water were used for UPLC separation. Extracts were separated using a Phenomenex Kinetex 2.6-mm C18 column (2.1 mm by 50 mm) using a 9 min, linear water-ACN gradient (from 98:2 to 2:98 % water/ACN) containing 0.1 % FA at a flow rate of 0.5 ml/min. The mass spectrometer was operated in data-dependent positive ion mode, automatically switching between full-scan MS and MS/MS acquisitions. Full-scan MS spectra (*m/z* 50 to 1500) were acquired in the TOF-MS, and the top five most intense ions in a particular scan were fragmented via collision-induced dissociation (CID) using the stepping function in the collision cell. Data for PA mix, a set of *P. aeruginosa* secondary metabolite external standards, were acquired under identical conditions. Bruker Daltonics CompassXport was used to apply lock mass calibration and convert the data from proprietary to open-source format. MZmine (version 2.53) [40] was used to perform feature finding. Identification of features in the molecular network as metabolites [41] was accomplished by comparing the experimental data (exact mass, MS/MS fragmentation, and retention time) to (i) the data acquired for the PA Mix standards (level 1 annotation) or (ii) reported structural data [42,43] for features with MS/MS spectral matches to the GNPS libraries [44] (level 2 annotation) using GNPS Dashboard [45]. Principal components analysis was performed using MetaboAnalyst 5.0 [46]. Comparison of relative abundance of select *P. aeruginosa* secondary metabolites between samples was performed using GraphPad Prism (version 9.3.1).

2.9. Effect of P. aeruginosa cell-free supernatant on S. aureus

Mono- (PAO1) or dual-species (PAO1 + *S. aureus* ATCC25923) cultures were grown following the conditions described in Protocol #2, with a ratio of 1 Sa to 0.064 Pa for the dual-species culture. After 72 h incubation, supernatants were collected, mixed by vigorous pipetting, and centrifuged at 12,000 g for 20 min at 4 °C. The collected supernatants were then filtered (0.22 μm-pore-size filter (Merck Millipore)) and stored at −20 °C until use. A disk diffusion assay against *S. aureus* was performed. Briefly, paper disks were impregnated with supernatant and allowed to dry. The disks were placed on trypticase soy agar covered in a lawn of *S. aureus*. Plates were incubated for 24 h at 37 °C and inhibition was assessed visually.

2.10. Determination of the MIC for P. aeruginosa secondary metabolites against S. aureus

Minimum Inhibitory Concentrations (MIC) were determined in MHB-Ca using the microdilution method according to guidelines established by the Institute for Clinical and Laboratory Standards. The initial MIC, determined based on 2-fold successive dilutions, was used as a baseline and subsequent dilutions were made at 8 μg/mL intervals. 100 μL of secondary metabolites solutions diluted in MHB-Ca were sequentially added to 100 μL of *S. aureus* (~10^6 CFU/mL) in a concentration gradient to obtain a more accurate MIC.

2.11. Effect of P. aeruginosa secondary metabolites on S. aureus biofilms

S. aureus at a concentration of approximately 10^7 CFU/mL was incubated for 2 h in MHB-Ca. Following incubation, the medium was removed and replaced with fresh ASM + containing 50 μg/mL of pyocyanin or rhamnolipids (Sigma-Aldrich). Plates were incubated for 24 h, after which CFU and biomass were quantified.

2.12. Statistical analyses

GraphPad Prism® version 10.2.1 (GraphPad Software, Inc., San Diego, CA) was used. In most cases, multiple comparisons were performed using one-way or two-ways ANOVA with Tukey post-hoc tests after checking for normality of the data distribution; values that are significantly different ($p < 0.05$) were marked by stars (one-way ANOVA) or different letters (2-way ANOVA). Statistical tests, including number of replicates, of individual experiments are summarized in figure legends.

3. Results

3.1. Development of a dual-species co-culture model in ASM+ with reference strains

Several protocols for the establishment of *S. aureus* - *P. aeruginosa* dual-species biofilms have been developed [16,33,47–49]. However, these protocols were created using traditional laboratory media.

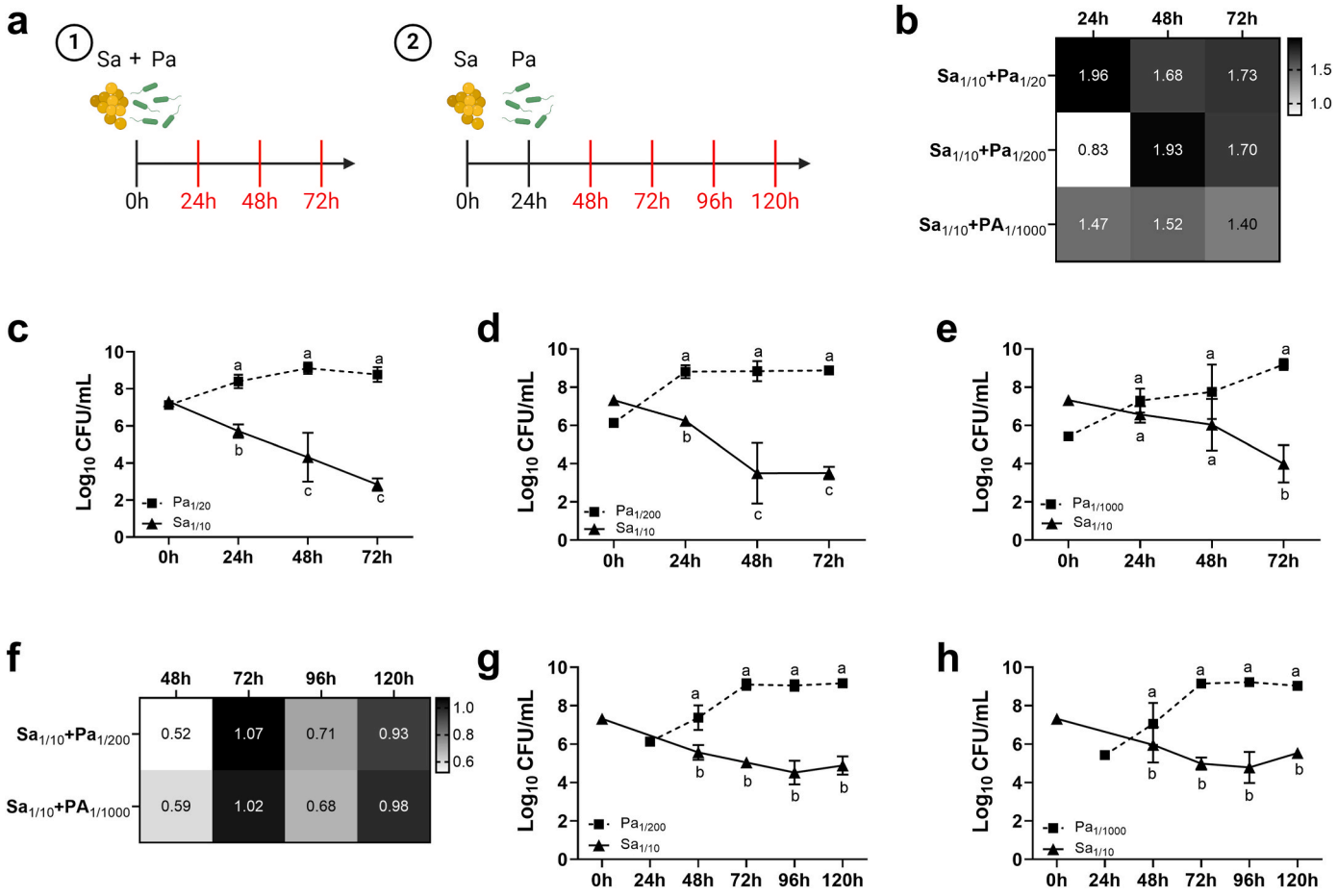

Fig. 1. Dual species *P. aeruginosa* and *S. aureus* co-culture method development. (a) Inoculation protocol schematic for dual species co-cultures in ASM+. For protocol #1, *S. aureus* ATCC25923 (Sa) and *P. aeruginosa* PAO1 (Pa) were inoculated simultaneously into ASM+ from OD_{620nm} 0.5 at three dilution ratios (Sa:Pa): 1/10:1/20, 1/10:1/200, or 1/10:1/1000 in 96 wells plates and incubated together for a duration of 72 h. Biofilm biomass and viable cell counts (CFU/mL) were measured at 24, 48, and 72 h post-inoculation. For protocol #2, inoculation of Sa and Pa was staggered. A 1/10 dilution of OD_{620nm} 0.5 Sa was inoculated into ASM+ and allowed to incubate. At 24 h, a 1/200 or 1/1000 dilution of OD_{620nm} 0.5 Pa was inoculated into the wells. The co-culture was incubated together for 96 h (120 h post Sa inoculation). Biofilm biomass and viable cell counts (CFU/mL) were measured at 48 h, 72 h, 96 h, and 120 h post Sa inoculation. Created using BioRender. **(b)** Biofilm biomass of Pa-Sa co-cultures grown according to protocol #1 labeled with mean. **(c–e)** CFU/mL of Pa (open squares) and Sa (filled triangles) from (c) $Sa_{1/10}$:$Pa_{1/20}$, (d) $Sa_{1/10}$:$Pa_{1/200}$; and (e) $Sa_{1/10}$:$Pa_{1/1000}$ co-cultures grown according to protocol #1. Values are means ± SEM from 3 or 4 independent experiments performed in triplicate. Statistical significance ($p < 0.05$) of CFU/mL of each species over time (two-way ANOVA with Tukey's multiple comparisons test) is indicated by letters. **(f)** Biofilm biomass of Pa-Sa co-cultures grown according to protocol #2 labeled with mean. **(g–h)** CFU/mL of Pa (open squares) and Sa (filled triangles) from (g) $Sa_{1/10}$:$Pa_{1/200}$; and (h) $Sa_{1/10}$:$Pa_{1/1000}$ co-cultures grown according to protocol #2. Values are means ± SEM from 3 or 4 independent experiments performed in triplicate. Statistical significance ($p < 0.05$) of CFU/mL of each species over time (two-way ANOVA with Tukey's multiple comparisons test) is indicated by different letters.

Therefore, we tested the ability of the reference strains *P. aeruginosa* PAO1 and *S. aureus* ATCC25923 to establish dual-species biofilms in ASM + [28,32] using two distinct methods. In protocol #1 (Fig. 1a), *S. aureus* ATCC25923 and *P. aeruginosa* PAO1 were co-inoculated in 96-well plates for 72 h, with SaATCC25923 inoculum maintained at ~2.1 x 10^7 CFU/mL (1:10 dilution of $OD_{620\ nm}$ = 0.5) and PAO1 inoculum varying between 20-, 200-, and 1000-fold dilutions of $OD_{620\ nm}$ = 0.5 (representing 1.35 × 10^7, 1.35 × 10^6, and 2.7 × 10^5 CFU/mL, respectively). Biofilm biomass and viable cell counts of PAO1 and SaATCC25923 were measured every 24 h (Fig. 1). In co-cultures

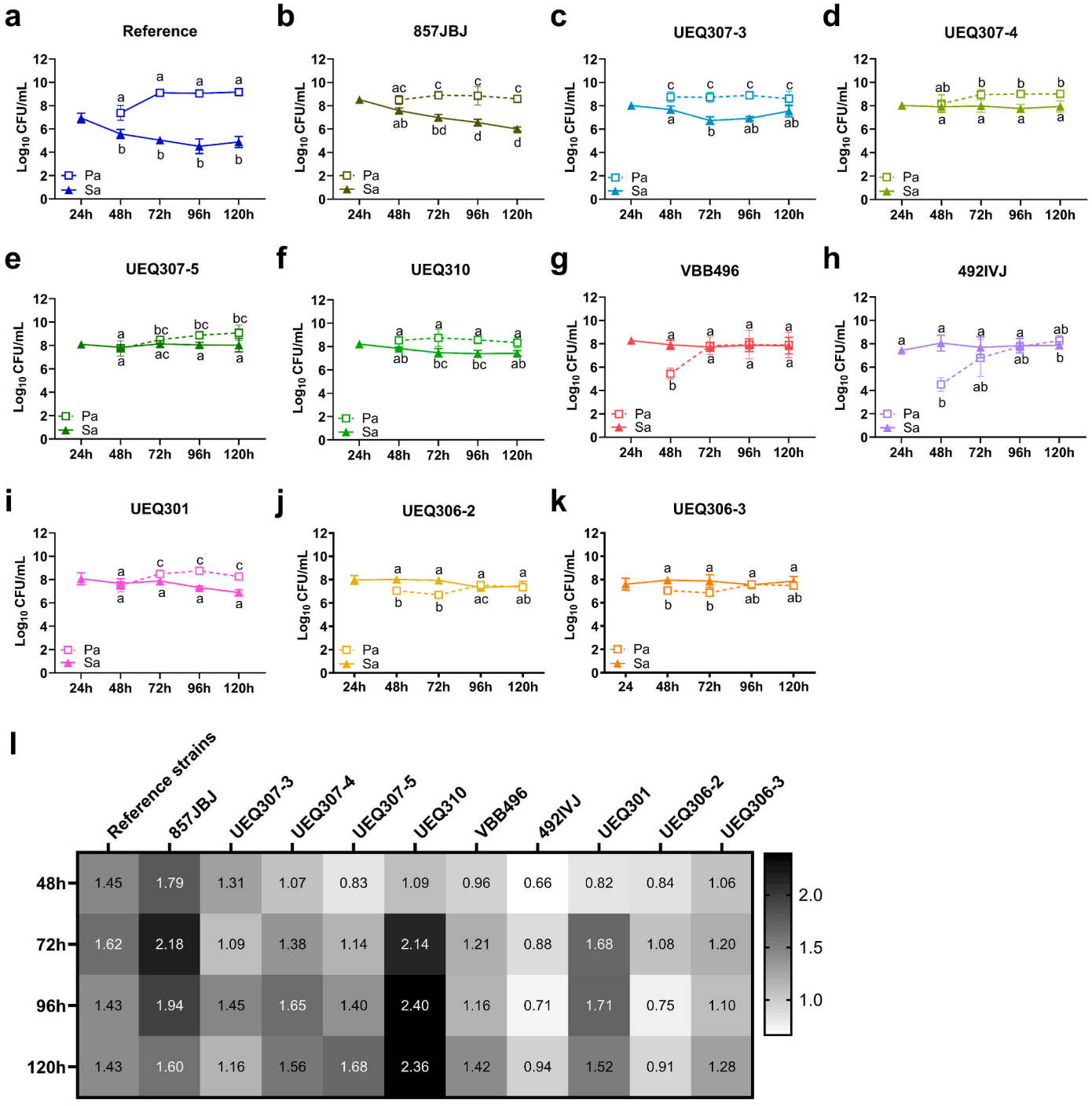

Fig. 2. Viable cell counts (CFU/mL) and biofilm biomass of *P. aeruginosa* (Pa) and *S. aureus* (Sa) co-isolate co-culture grown in ASM + using protocol #2. (a–k) CFU/mL of Pa (open squares) and Sa (filled triangles) recovered temporally from ASM + cultures: (a) Reference strains Pa PAO1 and SaATCC25923 (blue); (b) Pa857JBJ (pigmented non-mucoid) and Sa857JBJ (olive green); (c) PaUEQ307-3 (pigmented non-mucoid) and SaUEQ307 (robin's egg blue); (d) PaUEQ307-4 (pigmented non-mucoid) and SaUEQ307 (citrus green); (e) PaUEQ307-5 (pigmented non-mucoid) and SaUEQ307 (green); (f) PaUEQ310 (pigmented mucoid) and SaUEQ310 (lime); (g) PaVBB496 (non-pigmented mucoid) and SaVBB496 (coral red); (h) Pa492IVJ (non-pigmented mucoid) and Sa492IVJ (light slate blue); PaUEQ301 (non-pigmented mucoid) and SaUEQ301 (pink); PaUEQ306-2 (SCV) and SaUEQ306 (gold); (k) PaUEQ306-3 (SCV) and SaUEQ306 (orange). Values are means ± SEM from 3 or 4 independent experiments performed in triplicate. Statistical significance ($p < 0.05$) of CFU/mL of each species over time (two-way ANOVA with Tukey's multiple comparisons test) is indicated by different letters. **(l)** Biofilm biomass from co-isolate pairs from (a–k) labeled with mean. (For interpretation of the references to colour in this figure legend, the reader is referred to the Web version of this article.)

inoculated with 20-fold (Fig. 1c) and 200-fold (Fig. 1d) dilutions of PAO1, *P. aeruginosa* CFU/mL remained stable over time (8.4–8.8 $\log_{10}$ CFU/mL) after an initial 1–2 $\log_{10}$ increase at 24 h from initial inoculum levels. Co-cultures inoculated with 1000-fold dilutions (Fig. 1e) of PAO1 reached 9.2 $\log_{10}$ CFU/mL at 72 h. In all co-cultures, *S. aureus* counts were 1–1.5 $\log_{10}$ lower within 24h of inoculation and decreased over time; this effect was more rapid when PAO1 inoculum was higher. Despite lower biofilm biomass measured from co-cultures containing the 200-fold dilution of PAO1 at 24 h, it reached similar levels at 48 and 72 h in all conditions (Fig. 1b).

As protocol #1 did not support co-existence of SaATCC25923 with PAO1, protocol #2 was tested. In protocol #2 (Fig. 1a), SaATCC25923 was inoculated at ~2.1×10^7 CFU/mL (1:10 dilution of $OD_{620} = 0.5$) and incubated for 24 h prior to addition of 1.35×10^6, and 2.7×10^5 CFU/mL PAO1 (200- and 1000-fold dilutions of $OD_{620\ nm} = 0.5$, respectively). Under these conditions, pre-inoculation with *S. aureus* enabled its stable co-existence with both the 200-fold (Fig. 1g) and 1000-fold (Fig. 1h) dilutions of PAO1 at 72 h. After an initial 1.5–2 $\log_{10}$ decrease in CFU/mL, *S. aureus* recovery was maintained at ~5.0×10^5 CFU/mL regardless of PAO1 inoculum. In both conditions, PAO1 gained 3–3.5 $\log_{10}$ CFU/mL after inoculation, reaching stability at 72 h (Fig. 1g and h). No remarkable differences in biofilm biomass were measured between the different PAO1 inoculum concentrations or overtime (Fig. 1f). Based on these results, all further studies were performed following protocol #2 with *S. aureus* inoculated at a 1:10 dilution and *P. aeruginosa* inoculated at a 1:200 dilution of cultures normalized to an OD_{620} of 0.5.

3.2. Interrogation of dual-species clinical co-isolate co-existence in ASM+

As staggered inoculation of the reference strains in ASM + led to stable co-existence *in vitro*, we examined the ability of ten pairs of clinical *S. aureus* and *P. aeruginosa* co-isolates from the airways of people with CF (Table 1) to form stable co-culture over time (Fig. 2). The *P. aeruginosa* isolates were categorized into four groups based upon phenotype: pigmented non-mucoid (857JBJ, UEQ307-3, UEQ307-4, and UEQ307-5), pigmented mucoid (UEQ310), non-pigmented mucoid (VBB496, 492IVJ, and UEQ301), and small colony variant (SCV; UEQ306-2 and UEQ306-3). Regardless of phenotype, all *P. aeruginosa* isolates were viable in co-culture (Fig. 2b–k), with stable recovery over time (8.5–9 log10 CFU/mL), except for the mucoid non-pigmented isolates PaVBB496 (Fig. 2g) and Pa492IVJ (Fig. 2h), which gained ~2 and 3.5 $\log_{10}$ CFU/mL over time, respectively. Similarly, all *S. aureus* isolates were viable in co-culture (Fig. 2b–k), with stable recovery over time (8–8.5 $\log_{10}$ CFU/mL), with exception of Sa857JBJ (Fig. 2b) that had steadily decreasing recovery of viable cells over time, resulting in a 2.5 $\log_{10}$ reduction by 120 h. Although all co-cultures containing pigmented non-mucoid (Fig. 2b–e) and mucoid (Fig. 2f) *P. aeruginosa* isolates maintained a higher proportion of *P. aeruginosa* compared to *S. aureus*, co-cultures derived from the non-pigmented mucoid isolates PaVBB496 (Fig. 2g) and Pa492IVJ (Fig. 2h) and both SCV isolates (Fig. 2j–k) reached equivalent proportions of the two species by 72 or 96 h respectively.

Despite similar recovery of CFU/mL across all clinical co-isolate pairs, biofilm biomass varied (Fig. 2l). At 48 h, biofilm formation by most clinical isolate pairs was quantified at or below the levels produced by the PAO1-SaATCC25923 reference co-culture. Apart from co-isolate pairs 857JBJ, UEQ307-3, 492IVJ, UEQ306-2, and UEQ306-3, biofilm formation of the co-cultures increased over time. Co-isolate 857JBJ co-cultures produced consistently higher levels of biofilm compared to the reference co-cultures, despite decreased recovery of *S. aureus*. Although several mucoid *P. aeruginosa* isolates were included in this study, only co-cultures containing pigmented mucoid isolate PaUEQ310 produced markedly higher quantities of biofilm compared to the reference co-cultures containing non-mucoid PAO1.

Of note also, we observed that non-mucoid *P. aeruginosa* or pigmented-mucoid *P. aeruginosa* co-cultured with *S. aureus* formed aggregates in the medium as well as biofilms attached to the plastic surfaces. However, non-pigmented mucoid *P. aeruginosa* or small colony variants of *P. aeruginosa* predominantly form biofilms adhering on the plastic surface in co-culture with *S. aureus*.

3.3. S. aureus and P. aeruginosa biogeography in dual-species biofilm

To determine whether spatial organization contributed to the two predominant co-culture growth phenotypes displayed by the co-isolates, fluorescence confocal microscopy was applied to surface-attached biofilms formed by the representative UEQ307-3 and VBB496 co-isolate pairs on a submerged coverslip after 72 h (Fig. 3). The UEQ307-3 co-isolate pair represented the collection of isolate pairs wherein *P. aeruginosa* recovery was slightly higher than *S. aureus* and the VBB496 co-isolate pair represented those in which both species were equally represented at 120 h. The reference strain pair comprised of *S. aureus* ATCC25923 and PAO1 was used as control.

The three-dimensional organization of all three pairs was visually distinct. In the biofilm formed by the reference strains (Fig. 3a), PAO1 formed a lawn-like phenotype with microaggregate punctate locally distinct from the SaATCC25923 mushroom-like aggregate in the center of the coverslip. The biofilm formed by the UEQ307-3 co-isolate pair was comprised of two discrete layers (Fig. 3b), with PaUEQ307-3 forming a lawn-like phenotype distinct from the SaUEQ307-3 lawn. In contrast to the biofilms formed by the reference strains and the UEQ307-3 co-isolate pair, PaVBB496 and SaVBB496 formed co-localized aggregates throughout the biofilm (Fig. 3c). This spatial data revealed that the VBB496 co-isolate pair has reduced antagonism that enabled co-aggregation *in vitro* and may reflect cross-adaptation.

3.4. Interrogation of dual-species co-existence in ASM + cross-cultures

To investigate the cross-adaptation of the VBB496 co-isolate pair, we compared the recovery of PaVBB496 and SaVBB496 viable cell counts in monoculture, co-isolate co-culture, and cross-strain co-culture. For cross-strain co-culture, each species of the VBB496 co-isolate pair were cultured with either the appropriate reference strain (PAO1 or SaATCC25923) or the companion strain from the UEQ310 co-isolate pair. The UEQ310 co-isolate pair was chosen for this analysis because PaUEQ310 is a pigmented mucoid strain. As alginate has been shown to promote co-existence of *S. aureus* with *P. aeruginosa* [50], inclusion of PaUEQ310 in this experiment reduces the likelihood that the mucoid phenotype of PaVBB496 alone could explain cross-adaptation of the VBB496 co-isolate pair. Since PaUEQ310 is pigmented, but PaVBB496 is not, differences in cross-strain co-existence may provide insight into whether *P. aeruginosa* small molecule virulence factors toxic to *S. aureus* are mediating the interactions [21,51].

Recovery of SaVBB496 was similar from both mono- and co-cultures over time (Fig. 4a), except at 72 h, where cross-cultures of SaVBB496 with PAO1 and PaUEQ310 resulted in a 1 $\log_{10}$ decrease in *S. aureus* recovery compared to monoculture and co-isolate co-culture with PaVBB496. However, co-culture with its co-isolate PaVBB496 enabled maintenance of SaVBB496 at ~3×10^7 CFU/mL through 120 h. Unlike SaVBB496, PaVBB496 recovery varied between cultures (Fig. 4b). The viability of PaVBB496 was reduced in both mono- and co-culture with SaATCC25923 to below the limit of quantitation by 72 h, while co-culture with its co-isolate SaVBB496 and, to a lesser extent cross-culture with isolate SaUEQ310, enhanced or maintained PaVBB496 growth. Of co-cultures containing PaVBB496, biofilm biomass was most abundant in the VBB496 co-isolate pair and generally reflected the viability of PaVBB496 in the presence of different *S. aureus* partners (Fig. 4c). Conversely, all co-cultures containing SaVBB496 formed biofilms, with the most abundant biofilm biomass measured from the cross-culture pair of PaUEQ310-SaVBB496, likely due to the ability of PaUEQ310 to produce robust biofilms (Fig. 1l).

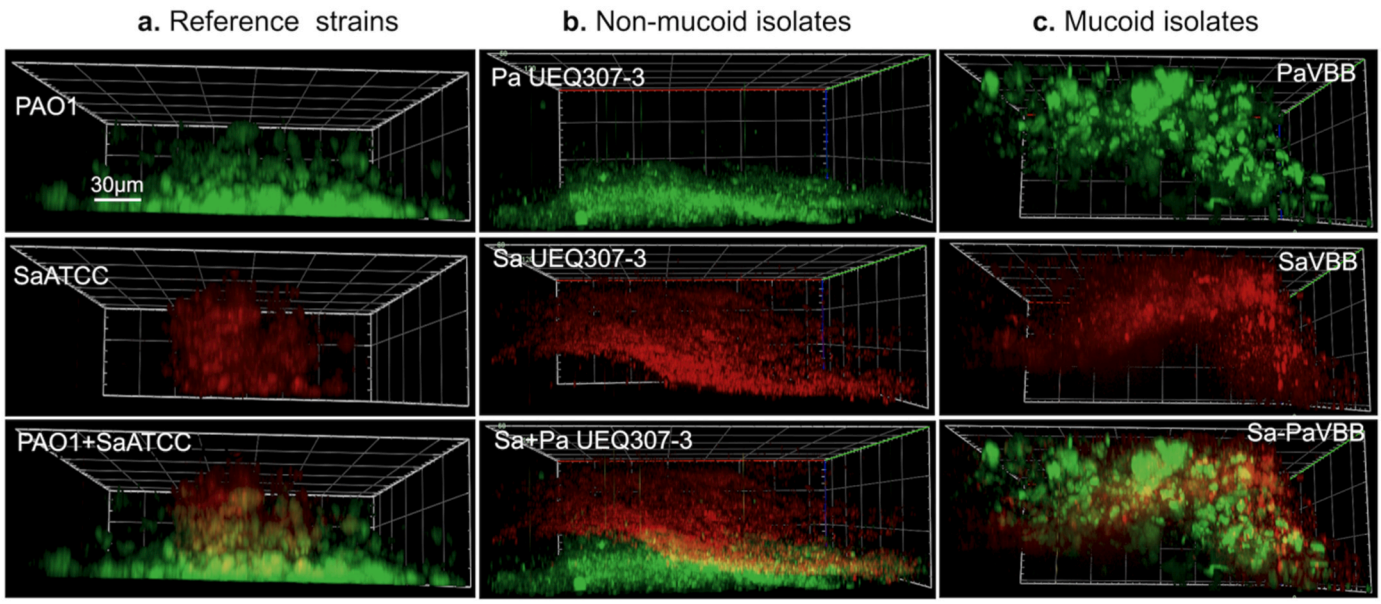

Fig. 3. Fluorescence in situ hybridization (FISH) images of *P. aeruginosa* (Pa) and *S. aureus* (Sa) dual-species biofilms. (a) Image of reference strains Pa PAO1 (green) and SaATCC25923 (red) co-culture. **(b)** Image of co-isolates pigmented non-mucoid PaUEQ307-3 (green) and SaUEQ307 (red). **(c)** Image of co-isolates non-pigmented mucoid PaVBB496 (green) and SaVBB496 (red) (named VBB on the figure). Top: Pa; middle: Sa, bottom: overlay. Bar, 30 μm. Note: z-stack constructed with the surface of the biofilm at the bottom of the image (slide) and the base of the biofilm at the top of the image (coverslip). (For interpretation of the references to colour in this figure legend, the reader is referred to the Web version of this article.)

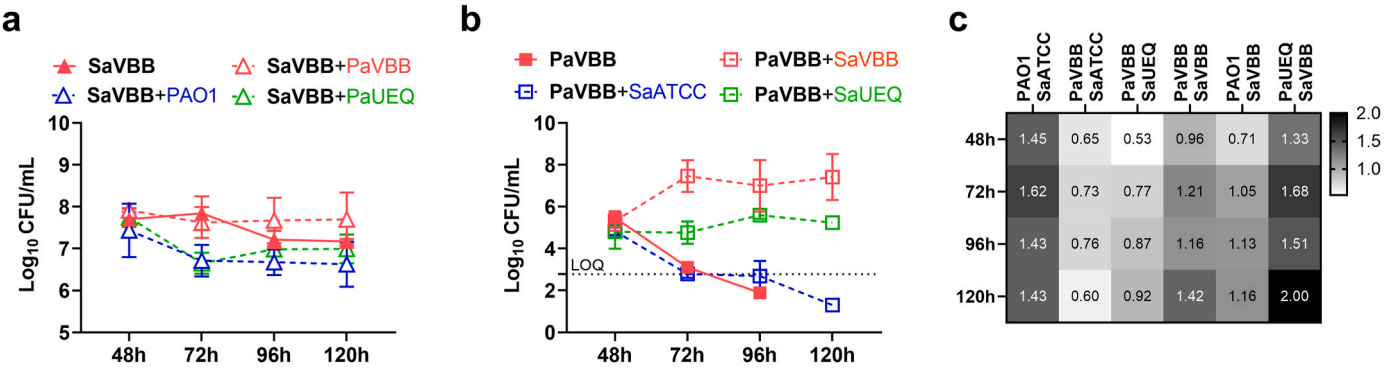

Fig. 4. Viable cell counts (CFU/mL) and biofilm biomass of cross-cultures of *P. aeruginosa* (Pa) and *S. aureus* (Sa) grown in ASM + using protocol #2. (a) CFU/mL of SaVBB496 recovered from monocultures (filled coral red triangles), co-culture with PAO1 (open blue triangles), co-culture with PaVBB496 (open coral red triangles), and co-culture with PaUEQ310 (open lime triangles) over time. **(b)** CFU/mL of PaVBB496 recovered from monocultures (filled coral red squares), co-culture with SaATCC25923 (open blue squares), co-culture with SaVBB496 (open coral red squares), and SaUEQ310 (open lime squares). Statistical analysis: Data with different letters are significantly different from each other ($p < 0.05$) when comparing 2 different biofilms at the same time point (Two-way ANOVA followed by Tukey's multiple comparisons test) **(c)** Biofilm biomass from PaVBB496 and SaVBB496 co-isolate pair culture and cross-culture with reference and SaUEQ310 strains labeled with mean. The co-culture of the reference strains PAO1 and SaATCC25923 was used as positive control. (For interpretation of the references to colour in this figure legend, the reader is referred to the Web version of this article.)

3.5. Relative expression of virulence associated genes

The antagonistic interaction between *P. aeruginosa* and *S. aureus* is well characterized, with quorum sensing (QS) regulated secreted factors produced by *P. aeruginosa* playing an important role in mediating *S. aureus* inhibition [7,21,51–53]. As the co-isolate VBB496 pair successfully co-existed in ASM+, we hypothesized that PaVBB496 demonstrated reduced production of QS regulated virulence factors. To test this hypothesis, qRT-PCR was used to measure the relative gene expression of *lasI, pvdS,* and *pqsL* in the 72 h biofilms formed by PaVBB496 in co-culture with SaVBB496 or SaATCC29523 (Fig. 5a). The 72-h time point was chosen for this analysis to capture the differential growth between PaVBB496-SaVBB496 and PaVBB496-SaATCC25923 co--cultures (Fig. 4b). Due to the lack of viability of PaVBB496 in monoculture, it was not possible to compare gene expression between the co-cultures to the monoculture.

The transcription of *lasI, pvdS,* and *pqsL* was downregulated −1.9 to -4-fold in PaVBB496 when co-cultured with its co-isolate SaVBB496 compared to SaATCC25923. LasI is an acyl homo serine lactone (AHL) synthase that produces the QS metabolite N-(3-oxododecanoyl) homoserine lactone (3-oxo-C12-HSL) [54]. The AHL 3-oxo-C12-HSL binds to LasR, which induces dimerization and activates transcription of hundreds of genes. Historically, LasI/R has been considered the apex of the *P. aeruginosa* QS system [55] and is required for production of the anti-staphylococcal small molecule inhibitors pyocyanin (PYO), rhamnolipids (RLs), and alkyl quinolone 2-heptyl-4-hydroxyquinoline N-oxide (HQNO) in *P. aeruginosa* model strains [54]. The alkyl quinolone (AQ) HQNO is a potent inhibitor of the *S. aureus* electron transport chain, and its production is dependent on the function of the FAD-dependent monooxygenase PqsL [6,42]. The iron-starvation sigma

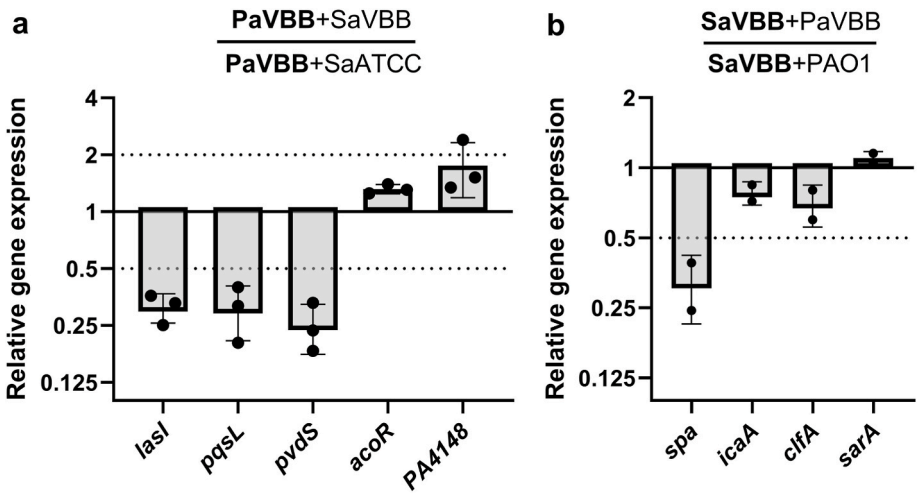

Fig. 5. Relative expression of genes involved in the interaction between *P. aeruginosa* (Pa) and *S. aureus* (Sa) at 72h co-incubation. (a) Relative expression of Pa genes *lasI*, *pqsL*, *pvdS*, *acoR*, and *PA4148* from PaVBB496 co-culture with its co-isolate SaVBB496 to PaVBB496 co-culture with the reference strain SaATCC25923. **(b)** Relative expression of Sa genes *spa*, *icaA*, *clfA*, and *sarA* from SaVBB496 co-culture with its co-isolate PaVBB496 to SaVBB496 co-culture with the reference strain PAO1. Data are mean ± SEM of 2–3 experiments in three replicates. A relative change of more than twofold in the expression level (limit highlighted by the dotted line) was considered significant.

factor PvdS regulates the transcription of genes involved in the biosynthesis of the siderophore pyoverdine (PVD) [56], known to contribute to inhibition of *S. aureus* in low-iron environments [6], as well as the proteinaceous virulence factors endoprotease (PrpL), alkaline protease (AprA) proteases, and exotoxin A [57]. Down-regulation of these three genes in PaVBB496 in co-culture with SaVBB496, but not SaATCC29523 suggested that presence of its co-isolate reduced the production of anti-staphylococcal virulence factors.

We also examined whether transcription of the acetoin catabolism operon (*aco*) was upregulated in PaVBB496 in co-culture with SaVBB496 compared to SaATCC25923 [58] (Fig. 5a). Acetoin, 3-hydroxybutanone, is produced by *S. aureus* CF clinical isolates and was detected from CF sputa [59,60]. Although accumulation of acetoin is toxic to *S. aureus*, it is catabolized by *P. aeruginosa* as a carbon source, likely contributing to the survival of both species in the CF airway [60]. The aco system is comprised of a transcriptional regulator AcoR (*PA4147*) and the operon PA4148-PA4153 [61]. Transcription of *acoR* and *PA4148* was slightly elevated in the PaVBB496-SaVBB496 co-culture, with a 1.3- and 1.75-fold increase, respectively, compared to PaVBB496-SaATCC29523. Our data tends to support previous findings that the aco system is more efficient with co-isolates [60].

As fluorescence confocal microscopy of the VBB496 co-isolate pair showed that they formed interspersed aggregates, we examined the transcription of *S. aureus* genes that mediate its own and *P. aeruginosa* biofilm formation, including *sarA*, *icaA*, *clfA*, and *spa* (Fig. 5b). Staphylococcal accessory regulator (SarA) is a global regulator of *S. aureus* virulence, including transcription of the *ica* operon and biofilm formation [62]. The icaADBC operon is essential in *S. aureus* biofilm formation by regulating the production of the exopolysaccharide poly-N-acetylglucosamine (PNAG; PIA) [63,64]. Adhesion proteins, including clumping factor A (ClfA) and Staphylococcal protein A (SpA), play an important role in *S. aureus* biofilm formation, particularly for strains that are unable to produce PNAG [64]. SpA has also been shown to inhibit biofilm formation, alter aggregate formation, and reduce sensitivity of some *P. aeruginosa* isolates to tobramycin through binding of the exopolysaccharide Psl or type IV pili [65,66]. In the co-isolate pair, SaVBB496 had 3.3-fold reduced transcription of *spa* compared to co-incubation with the reference strain PAO1. However, the expression of the other *S. aureus* genes was not significantly different in SaVBB496 co-culture with PaVBB496 or PAO1. Downregulation of *spa* by SaVBB496 in co-culture with PaVBB496 suggests *S. aureus* has decreased its metabolic processes unfavorable to its co-isolate.

3.6. Secondary metabolite profiling of PAO1 and PaVBB496 mono- and mixed species co-cultures

The relative gene expression data of select genes from the VBB496 co-isolate pair and cross-culture with the respective reference strains suggested that both PaVBB496 and SaVBB496 reduce antagonism with each other, supporting the observation of mutual adaptation in the CF airway. To measure whether there was a temporal response in *P. aeruginosa* small molecule virulence factor production between the VBB496 co-isolates and cross-pairs with the reference strains, secondary metabolite profiling [67,68] was applied to samples collected at the 48, 72, and 96 h (Fig. 6).

PAO1 secondary metabolites were detected at all three time points, with highest abundance measured from the 48 h samples (Fig. 6a). The levels of the redox active phenazines PYO and phenazine-1-carboxylic acid (PCA) measured from PAO1 monocultures decreased steadily over time, while the levels of alkyl quinolones 2-heptyl-4-quinolone (HHQ) and HQNO were highest in the 72 h samples (Fig. 6b). RL levels in these samples were maintained through the first two timepoints, with a marked lower level measured at 96 h (Fig. 6c). The siderophore PCH was not detected from the PAO1 monocultures likely due to the high level of iron in ASM + [39]. In PAO1-SaATCC25923 co-cultures, the levels of secondary metabolites were generally lower compared to PAO1 monocultures, with a shift towards reduced metabolite production over time (Fig. 6). Conversely, co-culturing PAO1 with SaVBB496 led to markedly higher levels of phenazines (PYO and PCA), alkyl quinolones (HHQ and HQNO), and PCH from the 48 h samples compared to both PAO1 monocultures and PAO1-SaATCC25923 co--cultures (Fig. 6a). Like the other conditions, PAO1 secondary metabolite levels from the PAO1-SaVBB496 co-cultures were lower in the 96 h samples compared to earlier timepoints (Fig. 6c), indicating temporal modulation. Notably, although PAO1 recovery from the 72 h co-cultures samples were ~2-$\log_{10}$ higher than from monocultures, the production of secondary metabolites was lower in co-culture than monocultures, confirming an adaptation of metabolic activity in the presence of *S. aureus* [48].

No secondary metabolites were detected from PaVBB496 monocultures (Fig. 6), likely due to lack of viability of PaVBB496 in ASM+ (Fig. 4b). Although PaVBB496 grew robustly in co-culture with

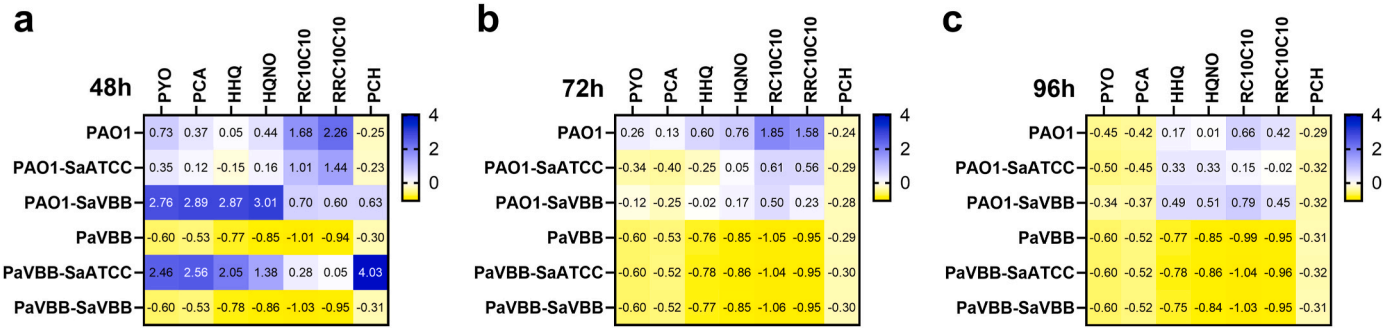

Fig. 6. *P. aeruginosa* PAO1 and PaVBB496 secondary metabolite profiles in mono- and co-culture. Heat map representation of normalized Z-scores of mean metabolite peak area of *P. aeruginosa* secondary metabolites known to mediate the interaction between *P. aeruginosa* and *S. aureus* across sample groups from **(a)** 48 h, **(b)** 72 h, and **(c)** 96 h samples. Data are labeled with the mean peak area of each metabolite $n = 9–12$ biological replicates. PYO, pyocyanin; PCA, phenazine-1-carboxamide; HHQ, 2-heptyl-4-quinolone; HQNO, 2-heptyl-4-hydroxyquinoline *N*-oxide; RC10C10, mono-rhamnolipid; RRC10C10, di-rhamnolipid; PCH, pyochelin.

SaVBB496 (Fig. 4b), secondary metabolites were not detected from these samples either (Fig. 6). However, co-culture of PaVBB496 with SaATCC25923 induced production of all secondary metabolites by PaVBB496 at 24 h (Fig. 6), with loss of metabolite detection over time corresponding to reduced viability of PaVBB496 with SaATCC25923 (Fig. 4b).

3.7. *SaVBB496 is less susceptible to P. aeruginosa secondary metabolites*

Cross-culture of SaVBB496 with PAO1 indicated that despite exposure to higher levels of *P. aeruginosa* secondary metabolites, the viability of this *S. aureus* strain was generally unaffected. A common explanation for the eradication of *S. aureus* by *P. aeruginosa* in *in vitro* systems is the lethality of the secondary metabolites PYO, PVD, RLs, and HQNO [7,21,51–53]. To determine whether SaVBB496 was better adapted to *P. aeruginosa* exoproducts than SaATCC25923, paper disks impregnated with PAO1 monoculture supernatant were tested for anti-staphylococcal activity using the disk diffusion assay (Fig. 7a). Although SaATCC25923 was inhibited by the PAO1 supernatant, SaVBB496 was not. Co-culture supernatant of PAO1 with SaATCC25923 yielded similar results, indicating that SaVBB496 is indeed less susceptible to *P. aeruginosa* secreted factors and co-culture did not alter the level of *P. aeruginosa* anti-staphylococcal activity. Evaluation of the antimicrobial activity of PYO, HQNO, RLs, and PVD against SaATCC25923 and SaVBB496 revealed that only PYO inhibited *S. aureus* growth, with SaVBB496 demonstrating a higher tolerance compared to SaATCC25923 (Fig. 7b–c).

4. Discussion

To study the clinically important co-existence of the opportunistic pathogens *P. aeruginosa* and *S. aureus*, many *in vitro* systems have been established. Although these two pathogens are often co-isolated from the airways of people with CF, their interactions *in vitro* are most often antagonistic, particularly when following the common practice of co-inoculating the two species at the same time [6,69–72]. This antagonism has been attributed to a myriad of factors, including inhibition of *S. aureus* by toxic metabolites produced by *P. aeruginosa* [7,16,21,51–53] and gradient concentrations of critical nutrients, such as oxygen and glucose, within co-cultured biofilms [72]. However, the antagonism of *S. aureus* and *P. aeruginosa* can be overcome by staggering the inoculation of the co-cultures and inoculating *S. aureus* first [16,73,74]. This approach more closely replicates the characteristics of *in vivo* co-infection of the CF airway, whereby *S. aureus* colonization precedes acquisition of *P. aeruginosa* [3] and may contribute to *P. aeruginosa* attachment [33]. Therefore, our goal was to implement the staggered inoculation method to investigate the cross-adaptation of *P. aeruginosa* and *S. aureus* CF airway isolates in ASM + [28,32], a medium that mimics the nutrient composition and viscoelastic properties of CF airway mucus.

The staggered cultivation strategy enabled successful co-existence of the laboratory reference strains PAO1 and SaATCC25923 in ASM+. Under our experimental conditions, PAO1 outcompeted SaATCC25923 in simultaneously inoculated mixed cultures regardless of the PAO1 starting inoculum, although lower concentrations of PAO1 led to delayed *S. aureus* killing. Using the staggered inoculation approach, the co-culture reached equilibrium within 24 h post-inoculation of PAO1 (72 h time point) with similar ratios of PAO1 and SaATCC25923 recovered through 120 h regardless of the PAO1 starting inoculum.

Remarkably, this staggered inoculation model system in ASM + proved applicable to a swath of CF airway *P. aeruginosa* and *S. aureus* co-isolate pairs, irrespective of a diverse set of *P. aeruginosa* phenotypes including mucoid, pigmented, and small colony variants. Measurement of microbial viability revealed that clinical co-isolates of *S. aureus* and *P. aeruginosa* mature into co-existence over time as three different growth phenotypes: constant *P. aeruginosa* recovery with decreasing *S. aureus* levels (857JBJ), stable co-culture with a higher proportion of *P. aeruginosa* (UEQ307-3, UEQ307-4, UEQ307-5, UEQ310, and UEQ301), and constant *S. aureus* recovery with increasing *P. aeruginosa* levels reaching equivalent CFU/mL by 96 h (VBB496, 492IVJ, UEQ306-2, and UEQ306-3). Notably, the recovery of *S. aureus* from the co-isolate pairs was higher than SaATCC25923 recovery from the reference pair co-culture, supporting the notion that *P. aeruginosa* and *S. aureus* cross-adapt *in vivo* resulting in reduced antagonism [22]. These results align well with existing literature demonstrating co-adaptation to the CF airway by *P. aeruginosa* and *S. aureus* co-isolates [14,50,60,69].

Overproduction of the exopolysaccharide alginate is typically associated with biofilm formation by *P. aeruginosa* [75]. However, biofilm biomass of the co-cultures was not associated with *P. aeruginosa* mucoid phenotype. The highest biofilm biomass was measured from the UEQ310 co-isolate pair, which includes a pigmented, mucoid *P. aeruginosa* strain. However, the co-isolate pairs comprised of non-pigmented mucoid *P. aeruginosa* strains (e.g., VBB496, 492IVJ, and UEQ301) did not produce more biofilm biomass than the pigmented non-mucoid strains. As recovery of *P. aeruginosa* and *S. aureus* was generally equivalent across all co-isolate cultures, bacterial viability was also not associated with biofilm biomass. The lack of coherence of our data to expected results may be due to differential alginate expression by the mucoid isolates, unexpected reversion to non-mucoid under our culture conditions, or lack of adherence of the cultures to the well plate.

Although plate-based assays provide an estimate of biofilm biomass, they do not capture the geographic distribution of the co-existing species. *In vivo*, it is thought that despite recovery from the same lobe of CF lungs, *P. aeruginosa* and *S. aureus* form discrete biofilm microcolonies that may reflect the presumed physical or chemical competition between the two species [29,30]. Here we observed that, depending on the

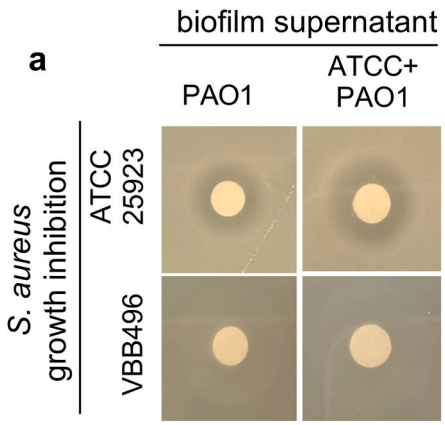

b

Exogenous QS products of *P. aeruginosa* (MIC [mg/L])				
S. aureus Strains	PYO	PVD	RLs	HQNO
ATCC 25923	16	≥1000	≥2000	≥1000
VBB496	24	≥1000	≥2000	≥1000

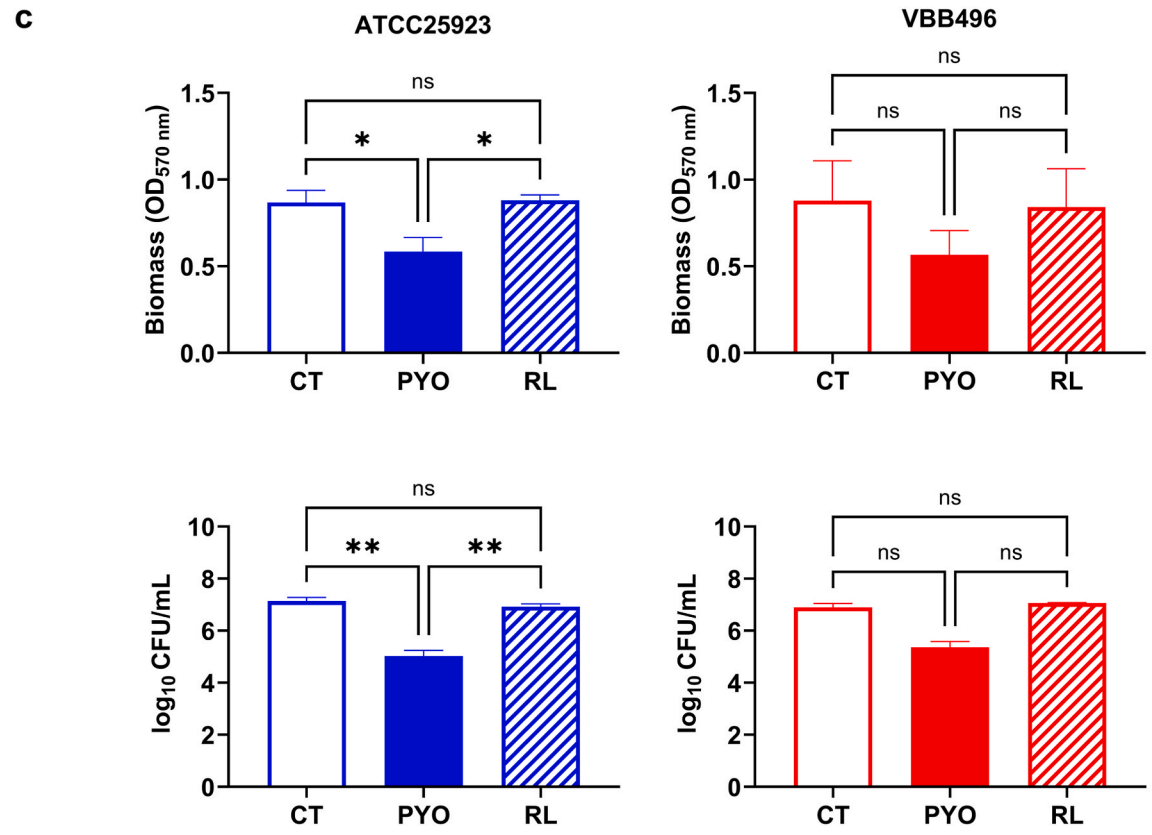

Fig. 7. Effect of *P. aeruginosa* exoproducts on *S. aureus*. **(a)** Disk diffusion assay of PAO1 and PAO1-SaATCC25923 supernatants against SaATCC25923 and SaVBB496. **(b)** Minimum inhibitor concentrations (MICs) of *P. aeruginosa* secondary metabolites known to inhibit *S. aureus,* including pyocyanin (PYO), pyoverdine (PVD), rhamnolipids (RL), and 2-heptyl-4-hydroxyquinoline *N*-oxide (HQNO). **(c)** Effect of 50 μg/mL pyocyanin (PYO) and rhamnolipids (RLs) on SaATCC25923 and SaVBB496 biofilm biomass and viable cell counts (CFU/mL) after 24 h of exposure. Data are mean ± SEM of two independent experiments with at least 3 replicates for biomass, and the mean ± SD one experiment in two replicates for CFU. Statistical analysis: ns, not significant; **, $p < 0.01$, using one-way ANOVA followed by Tukey's multiple comparisons test.

phenotype of *P. aeruginosa*, biofilms were mainly found as aggregates in the ASM + medium or adhering to the surface. *In vivo* studies suggest a localization essentially in the mucus of patients [76], but systematic observations with diverse phenotypes of *P. aeruginosa* are lacking in human samples. *In vitro* studies report for example that small-colony variants of *P. aeruginosa* are highly adherent on pneumocytes and suggest that this step may initiate colonization [77].

It is also unclear whether cross-adapted clinical isolates with interdependence for growth would have the same distribution. We were curious whether the VBB496 co-isolate pair, wherein PaVBB496 was dependent on the presence of SaVBB496 for survival in ASM+, would form distinct species-specific microcolonies. Unlike the reference strain pair as well as a pair of clinical co-isolates representing a more competitive pair (UEQ307-3), interspersion of the VBB496 co-isolates was clearly observed using fluorescence microscopy, further supporting cross-adaptation and cooperation.

For further insight into the co-adaptation of the VBB496 co-isolate pair, the isolates were subjected to cross-culture with reference strains or the UEQ310 co-isolates. Under these culture conditions, SaVBB496 was recovered from all cultures, with PAO1 and PaUEQ310 limiting and PaVBB496 enhancing its viability over time compared to monoculture. Conversely, PaVBB496 could only survive and proliferate when co-cultured with CF airway isolates and highest recovery was from co-culture with its co-isolate *S. aureus*. Reflective of the demonstrated

enhancement of *P. aeruginosa* viability in paired co-culture, the VBB496 co-isolate pair also formed higher biofilm biomass compared to the PaVBB496 cross-cultures with SaATCC25923 and SaUEQ310. Notably, the highest biofilm biomass was formed by cross-culture of SaVBB496 with PaUEQ310, but this observation likely reflects the ability of PaUEQ310 to form high levels of biofilm regardless of its *S. aureus* partner as evidenced by robust biofilm formation with its co-isolate SaUEQ310.

Co-inoculation of PaVBB496 with SaVBB496 enabled PaVBB496 to expand despite diminished viability in monoculture, suggesting that SaVBB496 provides a metabolic advantage. The lack of production of small molecule virulence factors by PaVBB496 evidenced by its non-pigmented appearance, lower expression of QS associated genes, and lack of secondary metabolites detected from the VBB496 co-isolate pair suggests that PaVBB496 may have disrupted las-dependent QS signaling. In model *P. aeruginosa* strains, LasI produces 3-oxo-C12-HSL, which binds to LasR and activate the transcription of virulence-associated genes, including most of the biosynthetic pathways of its secondary metabolites [78]. Mutations in *lasR* are common in *P. aeruginosa* CF airway isolates [79–81]. These *lasR* mutants over-produce nitric oxide, a compound highly toxic to *P. aeruginosa* leading to autolysis [82]. *S. aureus* has been shown to increase the growth of CF airway *P. aeruginosa lasR* mutants by detoxifying nitric oxide [82], likely as a part of its own adaptation to nitrosative stress from phagocytes [83]. This detoxification mechanism provides an explanation for why PaVBB496 is not viable in monoculture but formed stable co-cultures with CF isolates SaVBB496 and SaUEQ310 to varying degrees.

Intriguingly, despite lack of secondary metabolite production with SaVBB496, PaVBB496 secondary metabolites were detected from cross-culture with SaATCC25923. This result suggests that SaATCC25923 may produce a metabolite that is capable of inducing QS in PaVBB496. Recently, metabolic cross-feeding of citrate from *S. aureus* was shown to cause a *lasR* deletion mutant in the *P. aeruginosa* PA14 background to produce pyocyanin, likely through activation of RhlR-driven signaling [84]. The alteration in QS signaling due to carbon source availability was posited to increase *lasR* mutant fitness. However, the inability of SaATCC25923 to support PaVBB496 viability overtime suggests that the impetus for *P. aeruginosa* secondary metabolite production was not sufficient to overcome autolysis or inhibition by *S. aureus* under these conditions.

The ability of SaVBB496 to form stable cross-cultures is due, in part, to its reduced sensitivity to *P. aeruginosa* anti-staphylococcal secondary metabolites and down regulation of its expression of SpA, an inhibitor of *P. aeruginosa* biofilm formation and motility [65]. Notably, the metabolomics data also revealed a time-dependent component, with decreased levels *P. aeruginosa* secondary metabolites measured at later time points regardless of the presence of *S. aureus*. This result suggests that as *P. aeruginosa* acclimates to its environment, it may become less antagonistic to co-occurring *S. aureus*.

This work showcases the feasibility of cultivating *P. aeruginosa* and *S. aureus* under physiologically relevant conditions to understand their molecular interactions within the airways of people with CF. Although we focused on elucidating the interactions of a single co-isolate pair, this work illustrates the dynamic and multi-factorial interactions that dictate co-existence or antagonism between these two species. We anticipate that in-depth investigation of the interactions governing co-existence between the other co-isolate pairs in our study will reveal alternative mechanisms not captured in the VBB496 co-cultures. We also acknowledge some limitations of our model, including the fact we did not specifically examine the impact of pH or oxygen on biofilm formation or stability, that the observation we made are linked to the specific ratio between species we used to allow optimal growth, and that biofilms were grown in 96-well plates, which may have influenced their capacity to adhere to the surface.

In spite of the limitations inherent to any *in vitro* model, the system we implemented is highly adaptable to exploring some of the effects of CF airway environmental conditions, including nutrient availability and community composition, on the viability, biofilm formation, and metabolism of *P. aeruginosa* and *S. aureus* co-isolates. Further work integrating phenotypes, molecular profiles, and transcriptional analysis is required to clarify the diverse mechanisms that enable evolution of *P. aeruginosa* and *S. aureus* from competition to coexistence over chronicity of infection in the CF airway [85].

CRediT authorship contribution statement

Zhifen Wang: Writing – original draft, Methodology, Investigation, Formal analysis, Conceptualization. **Emily Giedraitis:** Writing – review & editing, Investigation, Formal analysis. **Christiane Knoop:** Writing – review & editing, Resources. **Daniel J. Breiner:** Writing – review & editing, Investigation, Formal analysis. **Vanessa V. Phelan:** Writing – original draft, Methodology, Funding acquisition, Formal analysis. **Françoise Van Bambeke:** Writing – original draft, Funding acquisition, Formal analysis, Conceptualization.

Declaration of competing interest

The authors declare that they have no known competing financial interests or personal relationships that could have appeared to influence the work reported in this paper.

Acknowledgments

Z.W. was recipient of a Chinese Scholarship Council (CSC) PhD grant and a grant from the King Baudouin Foundation (Fonds Forton) and the Belgian Mucovereniging/Association Muco. F.V.B. is research director from the Belgian Fonds de la Recherche Scientifique (FNRS-FRS). This work was supported by grants from the Belgian FNRS (grants J.0162.19, J.0177.23, andJ.0218.25) and the King Baudouin Foundation (Fonds Forton) and the Belgian Mucovereniging/Association Muco to F.V.B., and by National Institutes of Health grant R35 GM128690 and the L.S. Skaggs Professorship from ALSAM Foundation to V.V.P. The authors thank V. Mohymont, M. Scopa, and R. Tricot for dedicated technical assistance.

Appendix A. Supplementary data

Supplementary data to this article can be found online at https://doi.org/10.1016/j.bioflm.2025.100279.

Data availability

Data will be made available on request.

References

[1] Ratjen F, Bell SC, Rowe SM, Goss CH, Quittner AL, Bush A. Cystic fibrosis. Nat Rev Dis Primers 2015;1:15010. https://doi.org/10.1038/nrdp.2015.10.
[2] Shteinberg M, Haq IJ, Polineni D, Davies JC. Cystic fibrosis. Lancet 2021;397:2195–211. https://doi.org/10.1016/S0140-6736(20)32542-3. 10290.
[3] Cystic_Fibrosis_Foundation. 2020 patient registry annual data report. from, https://www.cff.org/sites/default/files/2021-10/2019-Patient-Registry-Annual-Data-Report.pdf; 2021.
[4] Lyczak JB, Cannon CL, Pier GB. Lung infections associated with cystic fibrosis. Clin Microbiol Rev 2002;15(2):194–222. https://doi.org/10.1128/CMR.15.2.194-222.2002.
[5] Barnabie PM, Whiteley M. Iron-mediated control of Pseudomonas aeruginosa-Staphylococcus aureus interactions in the cystic fibrosis lung. J Bacteriol 2015;197(14):2250–1. https://doi.org/10.1128/JB.00303-15.
[6] Filkins LM, Graber JA, Olson DG, Dolben EL, Lynd LR, Bhuju S, O'Toole GA. Coculture of Staphylococcus aureus with Pseudomonas aeruginosa drives S. aureus towards fermentative metabolism and reduced viability in a cystic fibrosis model. J Bacteriol 2015;197(14):2252–64. https://doi.org/10.1128/JB.00059-15.
[7] Nguyen AT, Oglesby-Sherrouse AG. Interactions between Pseudomonas aeruginosa and Staphylococcus aureus during co-cultivations and polymicrobial infections. Appl Microbiol Biotechnol 2016;100(14):6141–8. https://doi.org/10.1007/s00253-016-7596-3.

[8] Beaudoin T, Yau YCW, Stapleton PJ, Gong Y, Wang PW, Guttman DS, Waters V. Staphylococcus aureus interaction with Pseudomonas aeruginosa biofilm enhances tobramycin resistance. NPJ Biofilms Microbiomes 2017;3:25. https://doi.org/10.1038/s41522-017-0035-0.

[9] O'Brien S, Fothergill JL. The role of multispecies social interactions in shaping Pseudomonas aeruginosa pathogenicity in the cystic fibrosis lung. FEMS Microbiol Lett 2017;364(15):fnx128. https://doi.org/10.1093/femsle/fnx128.

[10] Pallett R, Leslie LJ, Lambert PA, Milic I, Devitt A, Marshall LJ. Anaerobiosis influences virulence properties of Pseudomonas aeruginosa cystic fibrosis isolates and the interaction with Staphylococcus aureus. Sci Rep 2019;9(1):6748. https://doi.org/10.1038/s41598-019-42952-x.

[11] Fischer AJ, Singh SB, LaMarche MM, Maakestad LJ, Kienenberger ZE, Pena TA, Stoltz DA, Limoli DH. Sustained coinfections with Staphylococcus aureus and Pseudomonas aeruginosa in cystic fibrosis. Am J Respir Crit Care Med 2021;203(3):328–38. https://doi.org/10.1164/rccm.202004-1322OC.

[12] Limoli DH, Hoffman LR. Help, hinder, hide and harm: what can we learn from the interactions between Pseudomonas aeruginosa and Staphylococcus aureus during respiratory infections? Thorax 2019;74(7):684–92. https://doi.org/10.1136/thoraxjnl-2018-212616.

[13] Limoli DH, Yang J, Khansaheb MK, Helfman B, Peng L, Stecenko AA, Goldberg JB. Staphylococcus aureus and Pseudomonas aeruginosa co-infection is associated with cystic fibrosis-related diabetes and poor clinical outcomes. Eur J Clin Microbiol Infect Dis 2016;35(6):947–53. https://doi.org/10.1007/s10096-016-2621-0.

[14] Briaud P, Bastien S, Camus L, Boyadjian M, Reix P, Mainguy C, Vandenesch F, Doleans-Jordheim A, Moreau K. Impact of coexistence phenotype between Staphylococcus aureus and Pseudomonas aeruginosa isolates on clinical outcomes among cystic fibrosis patients. Front Cell Infect Microbiol 2020;10:266. https://doi.org/10.3389/fcimb.2020.00266.

[15] Orazi G, O'Toole GA. Pseudomonas aeruginosa alters Staphylococcus aureus sensitivity to vancomycin in a biofilm model of cystic fibrosis infection. mBio 2017;8(4):e00873. https://doi.org/10.1128/mBio.00873-17. 00817.

[16] Woods PW, Haynes ZM, Mina EG, Marques CNH. Maintenance of S. aureus in Co-culture with P. aeruginosa while growing as biofilms. Front Microbiol 2018;9:3291. https://doi.org/10.3389/fmicb.2018.03291.

[17] Orazi G, Ruoff KL, O'Toole GA. Pseudomonas aeruginosa increases the sensitivity of biofilm-grown Staphylococcus aureus to membrane-targeting antiseptics and antibiotics. mBio 2019;10(4):e01501. https://doi.org/10.1128/mBio.01501-19. 01519.

[18] Yang L, Liu Y, Markussen T, Hoiby N, Tolker-Nielsen T, Molin S. Pattern differentiation in co-culture biofilms formed by Staphylococcus aureus and Pseudomonas aeruginosa. FEMS Immunol Med Microbiol 2011;62(3):339–47. https://doi.org/10.1111/j.1574-695X.2011.00820.x.

[19] Chew SC, Yam JKH, Matysik A, Seng ZJ, Klebensberger J, Givskov M, Doyle P, Rice SA, Yang L, Kjelleberg S. Matrix polysaccharides and SiaD diguanylate cyclase alter community structure and competitiveness of Pseudomonas aeruginosa during dual-species biofilm development with Staphylococcus aureus. mBio 2018;9(6):e00585. https://doi.org/10.1128/mBio.00585-18. 00518.

[20] Magalhaes AP, Lopes SP, Pereira MO. Insights into cystic fibrosis polymicrobial consortia: the role of species interactions in biofilm development, phenotype, and response to in-use antibiotics. Front Microbiol 2016;7:2146. https://doi.org/10.3389/fmicb.2016.02146.

[21] Price CE, Brown DG, Limoli DH, Phelan VV, O'Toole GA. Exogenous alginate protects Staphylococcus aureus from killing by Pseudomonas aeruginosa. J Bacteriol 2020;202(8):e00559. https://doi.org/10.1128/JB.00559-19. 00519.

[22] Camus L, Briaud P, Vandenesch F, Moreau K. How bacterial adaptation to cystic fibrosis environment shapes interactions between Pseudomonas aeruginosa and Staphylococcus aureus. Front Microbiol 2021;12:617784. https://doi.org/10.3389/fmicb.2021.617784.

[23] Planet PJ. Adaptation and evolution of pathogens in the cystic fibrosis lung. J Pediatric Infect Dis Soc 2022;11(Supplement_2):S23–31. https://doi.org/10.1093/jpids/piac073.

[24] Vyas HKN, Xia B, Mai-Prochnow A. Clinically relevant in vitro biofilm models: a need to mimic and recapitulate the host environment. Biofilms 2022;4:100069. https://doi.org/10.1016/j.bioflm.2022.100069.

[25] Branda SS, Vik S, Friedman L, Kolter R. Biofilms: the matrix revisited. Trends Microbiol 2005;13(1):20–6. https://doi.org/10.1016/j.tim.2004.11.006.

[26] Wimpenny J, Manz W, Szewzyk U. Heterogeneity in biofilms. FEMS Microbiol Rev 2000;24(5):661–71. https://doi.org/10.1111/j.1574-6976.2000.tb00565.x.

[27] Sun F, Qu F, Ling Y, Mao P, Xia P, Chen H, Zhou D. Biofilm-associated infections: antibiotic resistance and novel therapeutic strategies. Future Microbiol 2013;8(7):877–86. https://doi.org/10.2217/fmb.13.58.

[28] Diaz Iglesias Y, Wilms T, Vanbever R, Van Bambeke F. Activity of antibiotics against Staphylococcus aureus in an in vitro model of biofilms in the context of cystic fibrosis: influence of the culture medium. Antimicrob Agents Chemother 2019;63(7):e00602. https://doi.org/10.1128/aac.00602-19. 00619.

[29] Hogan DA, Willger SD, Dolben EL, Hampton TH, Stanton BA, Morrison HG, Sogin ML, Czum J, Ashare A. Analysis of lung microbiota in bronchoalveolar lavage, protected brush and sputum samples from subjects with mild-to-moderate cystic fibrosis lung disease. PLoS One 2016;11(3):e0149998. https://doi.org/10.1371/journal.pone.0149998.

[30] Wakeman CA, Moore JL, Noto MJ, Zhang Y, Singleton MD, Prentice BM, Gilston BA, Doster RS, Gaddy JA, Chazin WJ, Caprioli RM, Skaar EP. The innate immune protein calprotectin promotes Pseudomonas aeruginosa and Staphylococcus aureus interaction. Nat Commun 2016;7:11951. https://doi.org/10.1038/ncomms11951.

[31] Fazli M, Bjarnsholt T, Kirketerp-Moller K, Jorgensen B, Andersen AS, Krogfelt KA, Givskov M, Tolker-Nielsen T. Nonrandom distribution of Pseudomonas aeruginosa and Staphylococcus aureus in chronic wounds. J Clin Microbiol 2009;47(12):4084–9. https://doi.org/10.1128/JCM.01395-09.

[32] Sriramulu DD, Lunsdorf H, Lam JS, Romling U. Microcolony formation: a novel biofilm model of Pseudomonas aeruginosa for the cystic fibrosis lung. J Med Microbiol 2005;54(Pt 7):667–76. https://doi.org/10.1099/jmm.0.45969-0.

[33] Alves PM, Al-Badi E, Withycombe C, Jones PM, Purdy KJ, Maddocks SE. Interaction between Staphylococcus aureus and Pseudomonas aeruginosa is beneficial for colonisation and pathogenicity in a mixed biofilm. Pathog Dis 2018;76(1):fty003. https://doi.org/10.1093/femspd/fty003.

[34] O'Toole GA. Microtiter dish biofilm formation assay. J Vis Exp 2011;47:2437. https://doi.org/10.3791/2437.

[35] Ruiz-Sorribas A, Poilvache H, Kamarudin NHN, Braem A, Van Bambeke F. In vitro polymicrobial inter-kingdom three-species biofilm model: influence of hyphae on biofilm formation and bacterial physiology. Biofouling 2021:1–13. https://doi.org/10.1080/08927014.2021.1919301.

[36] Kempf VA, Trebesius K, Autenrieth IB. Fluorescent in situ hybridization allows rapid identification of microorganisms in blood cultures. J Clin Microbiol 2000;38(2):830–8. https://doi.org/10.1128/JCM.38.2.830-838.2000.

[37] Hogardt M, Trebesius K, Geiger AM, Hornef M, Rosenecker J, Heesemann Jr. Specific and rapid detection by fluorescent in situ hybridization of bacteria in clinical samples obtained from cystic fibrosis patients. J Clin Microbiol 2000;38(2):818–25. https://doi.org/10.1128/JCM.38.2.818-825.2000.

[38] Livak KJ, Schmittgen TD. Analysis of relative gene expression data using real-time quantitative PCR and the $2^{-\Delta\Delta CT}$ method. Methods 2001;25(4):402–8. https://doi.org/10.1006/meth.2001.1262.

[39] Neve RL, Carrillo BD, Phelan VV. Impact of artificial sputum medium formulation on Pseudomonas aeruginosa secondary metabolite production. J Bacteriol 2021;203(21):e0025021. https://doi.org/10.1128/JB.00250-21.

[40] Pluskal T, Castillo S, Villar-Briones A, Oresic M. MZmine 2: modular framework for processing, visualizing, and analyzing mass spectrometry-based molecular profile data. BMC Bioinf 2010;11:395. https://doi.org/10.1186/1471-2105-11-395.

[41] Sumner LW, Amberg A, Barrett D, Beale MH, Beger R, Daykin CA, Fan TW, Fiehn O, Goodacre R, Griffin JL, Hankemeier T, Hardy N, Harnly J, Higashi R, Kopka J, Lane AN, Lindon JC, Marriott P, Nicholls AW, Reily MD, Thaden JJ, Viant MR. Proposed minimum reporting standards for chemical analysis chemical analysis working group (CAWG) metabolomics standards initiative (MSI). Metabolomics 2007;3(3):211–21. https://doi.org/10.1007/s11306-007-0082-2.

[42] Lepine F, Milot S, Deziel E, He J, Rahme LG. Electrospray/mass spectrometric identification and analysis of 4-hydroxy-2-alkylquinolines (HAQs) produced by Pseudomonas aeruginosa. J Am Soc Mass Spectrom 2004;15(6):862–9. https://doi.org/10.1016/j.jasms.2004.02.012.

[43] Moree WJ, Phelan VV, Wu CH, Bandeira N, Cornett DS, Duggan BM, Dorrestein PC. Interkingdom metabolic transformations captured by microbial imaging mass spectrometry. Proc Natl Acad Sci U S A 2012;109(34):13811–6. https://doi.org/10.1073/pnas.1206855109.

[44] Wang M, Carver JJ, Phelan VV, Sanchez LM, Garg N, Peng Y, Nguyen DD, Watrous J, Kapono CA, Luzzatto-Knaan T, Porto C, Bouslimani A, Melnik AV, Meehan MJ, Liu WT, Crusemann M, Boudreau PD, Esquenazi E, Sandoval-Calderon M, Kersten RD, Pace LA, Quinn RA, Duncan KR, Hsu CC, Floros DJ, Gavilan RG, Kleigrewe K, Northen T, Dutton RJ, Parrot D, Carlson EE, Aigle B, Michelsen CF, Jelsbak L, Sohlenkamp C, Pevzner P, Edlund A, McLean J, Piel J, Murphy BT, Gerwick L, Liaw CC, Yang YL, Humpf HU, Maansson M, Keyzers RA, Sims AC, Johnson AR, Sidebottom AM, Sedio BE, Klitgaard A, Larson CB, P CAB, Torres-Mendoza D, Gonzalez DJ, Silva DB, Marques LM, Demarque DP, Pociute E, O'Neill EC, Briand E, Helfrich EJN, Granatosky EA, Glukhov E, Ryffel F, Houson H, Mohimani H, Kharbush JJ, Zeng Y, Vorholt JA, Kurita KL, Charusanti P, McPhail KL, Nielsen KF, Vuong L, Elfeki M, Traxler MF, Engene N, Koyama N, Vining OB, Baric R, Silva RR, Mascuch SJ, Tomasi S, Jenkins S, Macherla V, Hoffman T, Agarwal V, Williams PG, Dai J, Neupane R, Gurr J, Rodriguez AMC, Lamsa A, Zhang C, Dorrestein K, Duggan BM, Almaliti J, Allard PM, Phapale P, Nothias LF, Alexandrov T, Litaudon M, Wolfender JL, Kyle JE, Metz TO, Peryea T, Nguyen DT, VanLeer D, Shinn P, Jadhav A, Muller R, Waters KM, Shi W, Liu X, Zhang L, Knight R, Jensen PR, Palsson BO, Pogliano K, Linington RG, Gutierrez M, Lopes NP, Gerwick WH, Moore BS, Dorrestein PC, Bandeira N. Sharing and community curation of mass spectrometry data with global natural products social molecular networking. Nat Biotechnol 2016;34(8):828–37. https://doi.org/10.1038/nbt.3597.

[45] Petras D, Phelan VV, Acharya D, Allen AE, Aron AT, Bandeira N, Bowen BP, Belle-Oudry D, Boecker S, Cummings Jr DA, Deutsch JM, Fahy E, Garg N, Gregor R, Handelsman J, Navarro-Hoyos M, Jarmusch AK, Jarmusch SA, Louie K, Maloney KN, Marty MT, Meijler MM, Mizrahi I, Neve RL, Northen TR, Molina-Santiago C, Panitchpakdi M, Pullman B, Puri AW, Schmid R, Subramaniam S, Thukral M, Vasquez-Castro F, Dorrestein PC, Wang M. GNPS Dashboard: collaborative exploration of mass spectrometry data in the web browser. Nat Methods 2022;19(2):134–6. https://doi.org/10.1038/s41592-021-01339-5.

[46] Xia J, Psychogios N, Young N, Wishart DS. MetaboAnalyst: a web server for metabolomic data analysis and interpretation. Nucleic Acids Res 2009;37(Web Server issue):W652–60. https://doi.org/10.1093/nar/gkp356.

[47] Trizna EY, Yarullina MN, Baidamshina DR, Mironova AV, Akhatova FS, Rozhina EV, Fakhrullin RF, Khabibrakhmanova AM, Kurbangalieva AR, Bogachev MI, Kayumov AR. Bidirectional alterations in antibiotics susceptibility in Staphylococcus aureus-Pseudomonas aeruginosa dual-species biofilm. Sci Rep 2020;10(1):14849. https://doi.org/10.1038/s41598-020-71834-w.

[48] Reigada I, San-Martin-Galindo P, Gilbert-Girard S, Chiaro J, Cerullo V, Savijoki K, Nyman TA, Fallarero A, Miettinen I. Surfaceome and exoproteome dynamics in dual-species Pseudomonas aeruginosa and Staphylococcus aureus biofilms. Front Microbiol 2021;12:672975. https://doi.org/10.3389/fmicb.2021.672975.
[49] Oliveira IM, Gomes M, Gomes LC, Pereira MFR, Soares O, Mergulhao FJ. Performance of graphene/polydimethylsiloxane surfaces against S. aureus and P. aeruginosa single- and dual-species biofilms. Nanomaterials 2022;12(3):355. https://doi.org/10.3390/nano12030355.
[50] Limoli DH, Whitfield GB, Kitao T, Ivey ML, Davis Jr MR, Grahl N, Hogan DA, Rahme LG, Howell PL, O'Toole GA, Goldberg JB. Pseudomonas aeruginosa alginate overproduction promotes coexistence with Staphylococcus aureus in a model of cystic fibrosis respiratory infection. mBio 2017;8(2):e00186. https://doi.org/10.1128/mBio.00186-17. 00117.
[51] Noto MJ, Burns WJ, Beavers WN, Skaar EP. Mechanisms of pyocyanin toxicity and genetic determinants of resistance in Staphylococcus aureus. J Bacteriol 2017;199(17):e00221. https://doi.org/10.1128/JB.00221-17. 00217.
[52] Machan ZA, Taylor GW, Pitt TL, Cole PJ, Wilson R. 2-Heptyl-4-hydroxyquinoline N-oxide, an antistaphylococcal agent produced by Pseudomonas aeruginosa. J Antimicrob Chemother 1992;30(5):615–23. DOI: 2-Heptyl-4-hydroxyquinoline N-oxide, an antistaphylococcal agent produced by Pseudomonas aeruginosa.
[53] Buonocore C, Giugliano R, Della Sala G, Palma Esposito F, Tedesco P, Folliero V, Galdiero M, Franci G, de Pascale D. Evaluation of antimicrobial properties and potential applications of Pseudomonas gessardii M15 rhamnolipids towards multiresistant Staphylococcus aureus. Pharmaceutics 2023;15(2):700. https://doi.org/10.3390/pharmaceutics15020700.
[54] Miranda SW, Asfahl KL, Dandekar AA, Greenberg EP. Pseudomonas aeruginosa quorum sensing. Adv Exp Med Biol 2022;1386:95–115. https://doi.org/10.1007/978-3-031-08491-1_4.
[55] Gilbert KB, Kim TH, Gupta R, Greenberg EP, Schuster M. Global position analysis of the Pseudomonas aeruginosa quorum-sensing transcription factor LasR. Mol Microbiol 2009;73(6):1072–85. https://doi.org/10.1111/j.1365-2958.2009.06832.x.
[56] Cunliffe HE, Merriman TR, Lamont IL. Cloning and characterization of pvdS, a gene required for pyoverdine synthesis in Pseudomonas aeruginosa: PvdS is probably an alternative sigma factor. J Bacteriol 1995;177(10):2744–50. https://doi.org/10.1128/jb.177.10.2744-2750.1995.
[57] Tiburzi F, Imperi F, Visca P. Intracellular levels and activity of PvdS, the major iron starvation sigma factor of Pseudomonas aeruginosa. Mol Microbiol 2008;67(1):213–27. https://doi.org/10.1111/j.1365-2958.2007.06051.x.
[58] Kvich L, Crone S, Christensen MH, Lima R, Alhede M, Alhede M, Staerk D, Bjarnsholt T. Investigation of the mechanism and chemistry underlying Staphylococcus aureus' ability to inhibit Pseudomonas aeruginosa growth in vitro. J Bacteriol 2022;204(11):e0017422. https://doi.org/10.1128/jb.00174-22.
[59] Spanel P, Sovova K, Dryahina K, Dousova T, Drevinek P, Smith D. Do linear logistic model analyses of volatile biomarkers in exhaled breath of cystic fibrosis patients reliably indicate Pseudomonas aeruginosa infection? J Breath Res 2016;10(3):036013. https://doi.org/10.1088/1752-7155/10/3/036013.
[60] Camus L, Briaud P, Bastien S, Elsen S, Doleans-Jordheim A, Vandenesch F, Moreau K. Trophic cooperation promotes bacterial survival of Staphylococcus aureus and Pseudomonas aeruginosa. ISME J 2020;14(12):3093–105. https://doi.org/10.1038/s41396-020-00741-9.
[61] Liu Q, Liu Y, Kang Z, Xiao D, Gao C, Xu P, Ma C. 2,3-Butanediol catabolism in Pseudomonas aeruginosa PAO1. Environ Microbiol 2018;20(11):3927–40. https://doi.org/10.1111/1462-2920.14332.
[62] Valle J, Toledo-Arana A, Berasain C, Ghigo JM, Amorena B, Penades JR, Lasa I. SarA and not sigmaB is essential for biofilm development by Staphylococcus aureus. Mol Microbiol 2003;48(4):1075–87. https://doi.org/10.1046/j.1365-2958.2003.03493.x.
[63] Cramton SE, Gerke C, Schnell NF, Nichols WW, Gotz F. The intercellular adhesion (ica) locus is present in Staphylococcus aureus and is required for biofilm formation. Infect Immun 1999;67(10):5427–33. https://doi.org/10.1128/IAI.67.10.5427-5433.1999.
[64] Nguyen HTT, Nguyen TH, Otto M. The staphylococcal exopolysaccharide PIA - biosynthesis and role in biofilm formation, colonization, and infection. Comput Struct Biotechnol J 2020;18:3324–34. https://doi.org/10.1016/j.csbj.2020.10.027.
[65] Armbruster CR, Wolter DJ, Mishra M, Hayden HS, Radey MC, Merrihew G, MacCoss MJ, Burns J, Wozniak DJ, Parsek MR, Hoffman LR. Staphylococcus aureus protein A mediates interspecies interactions at the cell surface of Pseudomonas aeruginosa. mBio 2016;7(3):e00538. https://doi.org/10.1128/mBio.00538-16. 00516.
[66] Yung DBY, Sircombe KJ, Pletzer D. Friends or enemies? The complicated relationship between Pseudomonas aeruginosa and Staphylococcus aureus. Mol Microbiol 2021;116(1):1–15. https://doi.org/10.1111/mmi.14699.
[67] Depke T, Thoming JG, Kordes A, Haussler S, Bronstrup M. Untargeted LC-MS metabolomics differentiates between virulent and avirulent clinical strains of Pseudomonas aeruginosa. Biomolecules 2020;10(7):1041. https://doi.org/10.3390/biom10071041.
[68] Neve RL, Giedraitis E, Akbari MS, Cohen S, Phelan VV. Secondary metabolite profiling of Pseudomonas aeruginosa isolates reveals rare genomic traits. mSystems 2024;9(5):e0033924. https://doi.org/10.1128/msystems.00339-24.
[69] Baldan R, Cigana C, Testa F, Bianconi I, De Simone M, Pellin D, Di Serio C, Bragonzi A, Cirillo DM. Adaptation of Pseudomonas aeruginosa in Cystic Fibrosis airways influences virulence of Staphylococcus aureus in vitro and murine models of co-infection. PLoS One 2014;9(3):e89614. https://doi.org/10.1371/journal.pone.0089614.
[70] Pernet E, Guillemot L, Burgel PR, Martin C, Lambeau G, Sermet-Gaudelus I, Sands D, Leduc D, Morand PC, Jeammet L, Chignard M, Wu Y, Touqui L. Pseudomonas aeruginosa eradicates Staphylococcus aureus by manipulating the host immunity. Nat Commun 2014;5:5105. https://doi.org/10.1038/ncomms6105.
[71] Ammann CG, Nagl M, Nogler M, Coraça-Huber DC. Pseudomonas aeruginosa outcompetes other bacteria in the manifestation and maintenance of a biofilm in polyvinylchloride tubing as used in dental devices. Arch Microbiol 2016;198(4):389–91. https://doi.org/10.1007/s00203-016-1208-6.
[72] Cendra MdM, Blanco-Cabra N, Pedraz L, Torrents E. Optimal environmental and culture conditions allow the in vitro coexistence of Pseudomonas aeruginosa and Staphylococcus aureus in stable biofilms. Sci Rep 2019;9(1):1–17. https://doi.org/10.1038/s41598-019-52726-0.
[73] Magalhaes AP, Grainha T, Sousa AM, Franca A, Cerca N, Pereira MO. Viable but non-cultivable state: a strategy for Staphylococcus aureus survivable in dual-species biofilms with Pseudomonas aeruginosa? Environ Microbiol 2021;23(9):5639–49. https://doi.org/10.1111/1462-2920.15734.
[74] Magalhaes AP, Franca A, Pereira MO, Cerca N. Unveiling Co-infection in cystic fibrosis airways: transcriptomic analysis of Pseudomonas aeruginosa and Staphylococcus aureus dual-species biofilms. Front Genet 2022;13:883199. https://doi.org/10.3389/fgene.2022.883199.
[75] Hay ID, Gatland K, Campisano A, Jordens JZ, Rehm BH. Impact of alginate overproduction on attachment and biofilm architecture of a supermucoid Pseudomonas aeruginosa strain. Appl Environ Microbiol 2009;75(18):6022–5. https://doi.org/10.1128/AEM.01078-09.
[76] Bjarnsholt T, Jensen PO, Fiandaca MJ, Pedersen J, Hansen CR, Andersen CB, Pressler T, Givskov M, Hoiby N. Pseudomonas aeruginosa biofilms in the respiratory tract of cystic fibrosis patients. Pediatr Pulmonol 2009;44(6):547–58. https://doi.org/10.1002/ppul.21011.
[77] Haussler S, Ziegler I, Lottel A, Gotz FV, Rohde M, Wehmhohner D, Saravanamuthu S, Tummler B, Steinmetz I. Highly adherent small-colony variants of Pseudomonas aeruginosa in cystic fibrosis lung infection. J Med Microbiol 2003;52(Pt 4):295–301. https://doi.org/10.1099/jmm.0.05069-0.
[78] Azimi S, Klementiev AD, Whiteley M, Diggle SP. Bacterial quorum sensing during infection. Annu Rev Microbiol 2020;74:201–19. https://doi.org/10.1146/annurev-micro-032020-093845.
[79] Kostylev M, Kim DY, Smalley NE, Salukhe I, Greenberg EP, Dandekar AA. Evolution of the Pseudomonas aeruginosa quorum-sensing hierarchy. Proc Natl Acad Sci U S A 2019;116(14):7027–32. https://doi.org/10.1073/pnas.1819796116.
[80] Groleau MC, Taillefer H, Vincent AT, Constant P, Deziel E. Pseudomonas aeruginosa isolates defective in function of the LasR quorum sensing regulator are frequent in diverse environmental niches. Environ Microbiol 2022;24(3):1062–75. https://doi.org/10.1111/1462-2920.15745.
[81] O'Connor K, Zhao CY, Mei M, Diggle SP. Frequency of quorum-sensing mutations in Pseudomonas aeruginosa strains isolated from different environments. Microbiology (Read) 2022;168(12):001265. https://doi.org/10.1099/mic.0.001265.
[82] Hoffman LR, Richardson AR, Houston LS, Kulasekara HD, Martens-Habbena W, Klausen M, Burns JL, Stahl DA, Hassett DJ, Fang FC, Miller SI. Nutrient availability as a mechanism for selection of antibiotic tolerant Pseudomonas aeruginosa within the CF airway. PLoS Pathog 2010;6(1):e1000712. https://doi.org/10.1371/journal.ppat.1000712.
[83] Richardson AR, Libby SJ, Fang FC. A nitric oxide-inducible lactate dehydrogenase enables Staphylococcus aureus to resist innate immunity. Science 2008;319(5870):1672–6. https://doi.org/10.1126/science.1155207.
[84] Mould DL, Finger CE, Conaway A, Botelho N, Stuut SE, Hogan DA. Citrate cross-feeding by Pseudomonas aeruginosa supports lasR mutant fitness. mBio 2024;15(2):e0127823. https://doi.org/10.1128/mbio.01278-23.
[85] Camus L, Briaud P, Vandenesch F, Doleans-Jordheim A, Moreau K. Mixed populations and Co-infection: Pseudomonas aeruginosa and Staphylococcus aureus. Adv Exp Med Biol 2022;1386:397–424. https://doi.org/10.1007/978-3-031-08491-1_15.